

**Variations in esker morphology and internal architecture record time-transgressive deposition during ice margin retreat in Northern Ireland**

STOKER, B, LIVINGSTONE, S, BARR, I, RUFFELL, A, STORRAR, Robert <<http://orcid.org/0000-0003-4738-0082>> and ROBERSON, S

Available from Sheffield Hallam University Research Archive (SHURA) at:

<https://shura.shu.ac.uk/28540/>

---

This document is the Accepted Version [AM]

**Citation:**

STOKER, B, LIVINGSTONE, S, BARR, I, RUFFELL, A, STORRAR, Robert and ROBERSON, S (2021). Variations in esker morphology and internal architecture record time-transgressive deposition during ice margin retreat in Northern Ireland. Proceedings of the Geologists' Association. [Article]

---

**Copyright and re-use policy**

See <http://shura.shu.ac.uk/information.html>

# Variations in esker morphology and internal architecture record time-transgressive deposition during ice margin retreat in Northern Ireland

Ben J. Stoker<sup>a,b,\*</sup>, Stephen J. Livingstone<sup>b</sup>, Iestyn D. Barr<sup>c</sup>, Alastair Ruffell<sup>d</sup>, Robert D. Storrar<sup>e</sup>, Sam Roberson<sup>f</sup>

\*Corresponding author, email address: stokerb@natur.cuni.cz

<sup>a</sup> Department of Physical Geography and Geoecology, Charles University, Prague, Czechia

<sup>b</sup> Department of Geography, University of Sheffield, UK, South Yorkshire, Sheffield, Winter Street, S10 2TN

<sup>c</sup> Department of Natural Sciences, Manchester Metropolitan University, UK, Manchester, Oxford Road, M15 6BH

<sup>d</sup> School of Natural and Built Environment, Queens University Belfast, UK, Belfast, Elmwood Avenue, BT7 1NN

<sup>e</sup> Department of the Natural and Built Environment, Sheffield Hallam University, UK, Sheffield, Howard Street, S1 1WB

<sup>f</sup> Geological Survey of Northern Ireland, Dundonald House, Belfast, BT4 3SB, UK

Keywords: Eskers, Northern Ireland, morphology, sedimentology, deglaciation, meltwater

## Abstract

The architecture and evolution of the subglacial hydrological system plays a key role in modulating ice flow. Eskers provide an opportunity to understand subglacial hydrology at a broader perspective than contemporary studies. Recent research has established a morphogenetic classification for eskers, but these studies have been limited to topographically simple regions of a single ice sheet. We present an updated map of esker distribution in Northern Ireland based on 5 m resolution elevation data. We also present a high-resolution map of the glacial geomorphology of SW Northern Ireland, based on ~0.4 m resolution elevation data. Ground Penetrating Radar data from four sites along the >20 km long Evishanoran Esker system in central Northern Ireland are combined with geomorphological observations to provide insight into depositional processes and controls on esker formation. Esker architecture indicates two styles of deposition, including an initial high energy flow event in a subglacial conduit, and delta foreset deposition close to the ice sheet margin during ice margin retreat. These delta foreset deposits can be used to reconstruct former ice margins. We identify that local topographic complexity and geological structures (e.g. faults) are important controls on esker formation. The broad-scale esker architecture remains the same despite variable esker planform morphology, suggesting hydrological conditions alone cannot explain esker morphology. This study provides further evidence that morphogenetic relationships cannot be based solely on remote sensing data and must be supported by robust field observations, especially where post-glacial processes may distort esker morphology (e.g. peat infilling).

## 1.0 Introduction

The distribution of meltwater at the base of ice sheets influences ice motion by modulating basal sliding and deformation of sediments. The influence of water on ice flow depends on the architecture of the subglacial drainage network and how it evolves to accommodate water inputs (e.g. Budd et al., 1979; Alley et al., 1986; Iken and Bindshadler, 1986). Efficient low-pressure networks of discrete channels rapidly drain water to the margin and tend to reduce ice velocity (Hubbard and Nienow, 1997). Inefficient distributed networks (e.g. linked cavities, canals and a porous till layer) result in increased effective pressure, in turn leading to higher ice velocities (Röthlisberger, 1972; Schoof, 2010). Recent observations from beneath the Antarctic and Greenland ice sheets have implicated dynamic subglacial water systems in driving rapid ice-flow variations (Zwally et al., 2002; Bell et al., 2007; Stearns et al., 2008; Bartholomew et al., 2010; Davison et al., 2019).

For investigations of subglacial hydrological processes, the imprint of meltwater drainage, recorded on the beds of former ice sheets, has a clear advantage over data from contemporary ice sheets (e.g. borehole surveys) because it is possible to reconstruct the history of meltwater drainage over centennial to millennial time-scales and spatially over metres to hundreds of kilometres. These temporal and spatial scales not only allow a more complete understanding of the architecture and evolution of the subglacial drainage network but are relevant for informing numerical modelling experiments (cf. Greenwood et al., 2016; Hewitt & Creyts, 2019). Eskers are the depositional imprint of drainage through subglacial (R-channels), englacial or supraglacial channels (Price, 1969; Banerjee and McDonald, 1975; Gustavson and Boothroyd, 1987; Brennand, 2000) and are commonly found across the beds of former ice sheets (e.g. Storrar et al., 2014a; Stroeven et al., 2016; Clark et al., 2018). They typically comprise elongate ridges of glaciofluvially deposited sand and gravel that can extend tens to hundreds of kilometres, are usually arranged roughly parallel to former ice flow direction, and range from single ridges to more complex anabranching forms (e.g. Flint, 1930; Brennand, 1994; Burke et al., 2012; Storrar et al., 2015; Perkins et al., 2016). Esker geometry, distribution and sedimentary architecture have been widely used to reconstruct drainage pathways and infer past ice sheet dimensions and dynamics (e.g. Shreve, 1985; Dyke and Prest, 1987; Aylsworth and Shilts, 1989; Hebrand and Åmark, 1989; Clark and Walder, 1994; Brennand, 1994, 2000; Warren and Ashley, 1994; Margold et al., 2013; Storrar et al., 2013, 2014a; Livingstone et al., 2015). However, there is still considerable uncertainty over the genesis of eskers, including the extent to which they form time-transgressively or synchronously (e.g. Brennand, 2000; Makinen, 2003; Cummings et al., 2011); the magnitude and frequency of drainage (Burke et al., 2008, 2010, 2012; Livingstone et al., 2016; Drews et al., 2017); and the vertical position in the ice mass (i.e. supraglacial, englacial or subglacial) in which they are deposited (Price, 1969; Fitzsimmons, 1991; Perkins et al., 2016).

Understanding how eskers form is important for reconstructing palaeo-ice sheets and providing information on subglacial hydrological processes. In particular, the varied form and architecture of eskers is thought to be controlled by the hydrological properties of the channelised drainage system

(Burke et al., 2015; Storrar et al., 2015). For example, recent morpho-sedimentary studies of eskers in southern Alberta, Canada, and mapping of eskers emerging from the front of Breiðamerkurjökull, southeast Iceland, have related abundant meltwater and sediment supply to complex esker systems, and low sediment supply and either high or low meltwater abundance to single ridges of uniform geometry (Burke et al., 2015; Storrar et al., 2015, 2020). A barrier to understanding the formation of eskers at the ice sheet-scale is the relative dearth of sedimentological investigations of these long esker systems. Recent work (e.g. Burke et al., 2012; Perkins et al., 2013) has begun to address this using geophysical investigations of the sedimentary architecture of eskers formed beneath the Cordilleran Ice Sheet. To further investigate the relationship between ice sheet hydrology and esker properties, this paper combines detailed geomorphological, geophysical and sedimentological data to assess controls on the formation of a ~20 km long esker network in Northern Ireland (UK) whose morphology changes down-flow from a complex multi-ridge system to a large single ridge.

## 2.0 Background

### 2.1 Glacial history of Ireland

The early stages of the onset of the Irish Ice Sheet (~ 35 ka) were characterised by incursion of Scottish ice flowing in from the NE, which subsumed localised ice caps over Irish upland massifs (Colhoun, 1971; Clark and Meehan, 2001; Greenwood and Clark, 2009b). As Irish ice coalesced with western Scottish ice, the location of the dominant ice dispersal centres migrated to upland areas in the west of Ireland, exerting a strong control on ice flow patterns (Greenwood and Clark, 2009b). Heterogenous growth patterns led to ice sheet sectors reaching their maxima at different times. For example, the western margin reached its maximum position relatively early compared to the southern portion of the ice sheet (Ó Cofaigh and Evans, 2007; Greenwood and Clark, 2009b; Ó Cofaigh et al., 2019). The configuration of ice domes and the geomorphology of the Irish Ice Sheet required ice expansion onto the continental shelf, with the Last Glacial Maximum (LGM; 23 ka – 18 ka) resulting in almost complete terrestrial ice coverage across Ireland (Knight et al., 2004; Ó Cofaigh and Evans, 2007; Bradwell et al., 2008; Greenwood and Clark, 2009a,b; Clark et al. 2018).

Deglaciation in Ireland was characterised by the migration of competing ice divides, which resulted in a complex deglacial history (Knight, 2003, 2019; Greenwood, 2009b). The ice sheet fragmented as it retreated into upland dispersal centres such as the Connemara Mountains in Western Ireland and County Donegal to the north (Wilson *et al.*, 2019), or lowland ice domes situated in the Lough Neagh Basin and Omagh Basin (Fig. 1). Ice sheet retreat is thought to have been interspersed with asynchronous phases of localised ice advance or stagnation, likely related to the migration of ice divides (Knight, 1999; Knight, 2006; Clark *et al.*, 2012; Callard et al., 2020; Chiverrell *et al.*, 2020). Within central Northern Ireland, the two dominant LGM ice dispersal centres were situated in the Lough Neagh basin, and in the Sperrin Mountain range to the north (Fig. 1) (Knight, 1999). During this period, SW ice flow dominated from an ice dome in the NE Omagh Basin offshore towards Donegal Bay (Fig. 1), indicated

by an area of subglacial ribs across the Omagh Basin (Knight and McCabe, 1997). Subglacial ribs across central Northern Ireland often display modification or drumlinisation likely associated with changes in ice flow patterns and subglacial thermal regime (Knight, 1997; Knight and McCabe, 1997). An ice flow reversal occurred during deglaciation when the dominant ice dome over the Omagh Basin migrated SW to the Lower Lough Erne Basin, leading to NE ice flow forming a prominent esker system overlying the subglacial ribs (Knight, 2004). The regional retreat pattern to the SW is documented by a series of meltwater landforms, including eskers. A glacial lake formed between the retreating ice sheet margin and the Sperrin Mountains to the north, resulting in the formation of a series of deltas (Dardis, 1986). The final stages of deglaciation were characterised by localised mountain ice caps, with the last remnants of the Irish Ice Sheet likely located in the mountains of Donegal in the northwest (Greenwood and Clark, 2009b; Smith and Knight, 2011).

Research into the meltwater systems of Ireland has a long history stretching back to the late 19<sup>th</sup> century, and has concentrated on the origin of the large (up to 50 m high) ridges of the Esker Riada system in the Irish Midlands (Sollas, 1896; Gregory, 1912, 1921; Hinch, 1921; Flint, 1930). Theories on the origin of these eskers revolved around whether they were deposited by a sub- or supraglacial river system, or whether they represented deltaic glaciofluvial deposits (Gregory, 1921). More recently, studies have debated whether the Esker Riada system and associated glaciofluvial sediments were deposited by meltwater in an interlobate position, between two retreating ice masses (Warren and Ashley, 1994; Pellicer et al., 2012), or as part of a multi-phase model involving westerly ice sheet retreat, followed by a period of ice sheet readvance from the north (Delaney, 2001a, b, 2002; Delaney et al., 2018). The eskers of central Northern Ireland have been used to reconstruct the migration of ice domes and time-transgressive variations in the subglacial drainage system (Knight, 1997; 2019), but historically, there has been less research focused on them.

## *2.2 Regional Context and Landform Distribution*

Central Northern Ireland incorporates the Sperrin Mountains to the north and the Omagh Basin; a low elevation region of undulating topography, to the south (Fig. 1). The regional geology is varied, with a series of folded and faulted Palaeozoic sandstones and limestones to the south, and crystalline granites and gabbros to the north, with varying degrees of metamorphism across the Tyrone Igneous Complex (Knight, 1997; Chew *et al.*, 2008; Geological Survey Northern Ireland, 2016). A series of three large, subparallel fault lines trend NE-SW and define geological boundaries, while smaller faults with a variety of orientations are also prevalent (Geological Survey Northern Ireland, 2016).

A range of glacial landforms have been documented across the region, including meltwater channels, eskers, drumlins and subglacial ribs (Colhoun, 1970; Knight, 2003; Clark et al., 2018). Major moraines are largely absent across central Northern Ireland, being restricted to the present coastline and the continental shelf onto which the Irish Ice Sheet extended (Clark et al., 2018; Ó Cofaigh et al., 2019). An area of subglacial ribs dominates the lowland areas across Central Northern Ireland, with ridge

crestlines oriented perpendicular to SW ice flow during the LGM (Knight and McCabe, 1997; Knight, 2002). These subglacial ribs are commonly drumlinised or exhibit modification by meltwater, which may have been stored in the lowland area between ridge crestlines (Knight and McCabe, 1997; Knight, 2002, 2006). Alongside subglacial ribs, E-W orientated drumlins dominate the lowlands of the Omagh and Lough Erne basins (Knight, 1997, 2003). A prominent esker system located NE of the Lower Lough Erne Basin forms a series of bifurcating ridges in a meltwater valley dissecting the zone of subglacial ribs (Fig. 2a). This system was deposited under NE ice flow during deglaciation to the SW, contrasting with the SW ice flow responsible for the formation of the subglacial ribs (Knight, 2002). Therefore, these eskers represent a reversal of the hydraulic gradient as the ice dome situated over the Omagh Basin migrated towards the Lower Lough Erne Basin (Knight and McCabe, 1997).

The present study focuses on a >20 km long complex esker system in County Tyrone, Central Northern Ireland. The esker complex trends out of three meltwater channels cutting through the Fintona Hills to the south, and terminates near the Sperrin Mountains in the north (Figs. 1, 2 and 3). The NE sector was mapped in part by Gregory (1925) and termed the Evishanoran Esker. Early debate sought to identify whether deposition was associated with local ice masses from the east, or a larger ice mass from the southwest (Charlesworth, 1926; Gregory, 1926). Here we refer to the entire esker complex as the Evishanoran Esker, including newly mapped segments that were not documented in Gregory (1925). A series of eskers to the SW in the Fintona Hills were likely deposited during a later stage of deglaciation and form a meltwater routeway with the Evishanoran Esker (Knight, 2019).

### **3.0 Methods**

#### *3.1 Geomorphological mapping*

Comprehensive mapping of esker ridges was undertaken for the whole of Northern Ireland. Landform mapping was performed within ArcGIS 10.4.1, using a 5 m resolution digital elevation model (DEM) produced by the Land and Property Services Northern Ireland under MOU205, provided to Queens University Belfast. We also mapped all glacial landforms across the study area of SW Northern Ireland using a ~0.4 m resolution digital surface model (DSM) to provide geomorphological context of the area surrounding the Evishanoran Esker (Fig. 2).

Landform identification was based on morphology, association with other features and local topography. Esker crestlines were digitized as polylines to investigate their broad-scale distribution and morphological characteristics. Fan-shaped enlargements located at esker termini were classified as esker fans and digitized as polygons at the break of slope. The thalwegs of meltwater channels were digitized as polylines and classified as either subglacial or lateral according to the criteria set out by Greenwood *et al* (2007). All subglacial bedforms were mapped as polygons, including: subglacial ribs (ribbed moraine), drumlins, mega-scale glacial lineations, and streamlined bedrock features. Our mapping builds on earlier low-resolution mapping from Landsat and SPOT satellite imagery and field

surveys (Knight, 2003; Greenwood and Clark, 2009a), and has resulted in the creation of a comprehensive database of Northern Irish eskers, consistent with the NextMap 5 m resolution data used for the rest of the UK (Clark et al., 2018), and detailed mapping of glacial landforms in SW Northern Ireland at 0.4 m resolution.

### 3.2 Ground Penetrating Radar

Ground Penetrating Radar (GPR) data were acquired in August and November 2016. A total of ~1.8 km are presented here, including profiles along the crestlines of the eskers and cross profiles in a range of topographic contexts and for different esker forms. A 32-bit Mala Ground Explorer (GX) controller unit connected directly to a 160MHz GX shielded antenna on a rough terrain skid plate was used in August 2016. Radar profiles were acquired at a constant walking pace in a continuous, time-triggered shot mode using hyperstacking to reduce random noise. A Mala Ramac system consisting of a 4 m-long Rough Terrain Antenna, comprising in-line, unshielded transmitting and receiving antennas with a 1.5 m spacing and 100MHz centre frequency was used in November 2016. Collection of radar data was performed at a constant walking pace, in a time-triggered mode, with 16 stacks at a delay of 0.5-seconds. All radar survey lines were simultaneously mapped using a Leica CS15 differential Global Positioning System (dGPS) unit to topographically correct the profiles.

Processing of radar data was performed within REFLEXW v7.5.9, the proprietary software of Karl Sandmeier under licence number 401 provided to Queen's University, Belfast. A standard processing sequence was developed, using the following steps: static correction of time-zero drift, removal of low frequency signal saturation (dewow), application of gain to increase the visibility of reflections at depth, diffraction stack migration, background removal to reduce antenna ringing, bandpass filtering and topographic correction with the associated dGPS trace, finally radargrams were plotted in MatLab v9.1.0.441655 (Neal, 2004; Cassidy and Jol, 2009). A velocity of 0.1 m/ns for migration was used, consistent with exposures of eskers in sand extraction pits, hillside scars and road-cuts (see Section 3.3) (Russell et al., 2001; Pellicer et al., 2012; Livingstone et al., 2016). GPR profiles were interpreted by identifying high-amplitude reflectors indicative of bounding surfaces between radar facies. Six radar facies (*sensu* Gawthorpe *et al.*, 1993) were differentiated based upon depositional characteristics, including associations with sediment facies identified from exposures in the field and the broad characteristics of reflectors within a unit (Table 1). Lateral discontinuities and offset reflectors were interpreted as geological faults (e.g. Fiore et al., 2002).

### 3.3 Sedimentology

Gravel pit exposures adjacent to, and below, the GPR profiles were investigated to provide an insight into the flow conditions responsible for ridge formation in the Evishanoran Esker, and to provide ground-truthing for the interpretation of radargrams. Four sediment exposures were logged within the complex, multi-ridge system and the simple, single-ridge system (Fig. 2). Scaled sediment logs were drawn to record stratigraphic data, including details on the sedimentary structures, texture, and the unit

characteristics, such as bed geometry and contacts. Lithofacies were based on Evans and Benn (2004). Clast macrofabric and palaeoflow indicators (e.g. ripples) supplemented stratigraphic logs (Miall, 1985).

## **4.0 Results and interpretations**

### *4.1 Glacial Geomorphology*

A complete map of the glacial meltwater landforms of Northern Ireland is presented in Figure 2a. The map contains 457 esker ridges, totalling 220 km in length, compared to 63 esker ridges (40 km) detailed for this region in the BRITICE v2 database (Clark *et al.*, 2018). Esker distribution is heterogeneous, with the majority concentrated along a NE-SW axis to the south of the Sperrin Mountains and a > 20 km long N-S trending esker system to the north of the Lough Neagh Basin. Meltwater channels most commonly occur near upland regions (Fig. 2a). Meltwater channels have been documented by previous mapping efforts and are ubiquitous across Northern Ireland (Charlesworth, 1924; Colhoun, 1970; Knight, 2006; Greenwood and Clark, 2009a).

We present a detailed map of the glacial geomorphology of SW Northern Ireland in Figure 2b, including moraines, meltwater channels (lateral and subglacial), eskers and subglacial bedforms (lineations and ribs). To the south of the Sperrin Mountains, a complex system of over 80 ridges form the Evishanoran Esker system, spanning > 20 km and demonstrating considerable variation in morphology over its length (Fig. 2 and 3). The esker system is oriented SW-NE, broadly aligned with an area of subglacial ribs. Across this region, further glaciofluvial landforms associated with the esker system are observed. Most notably, the SW sector is associated with a series of subglacial meltwater channels cut into a slope that trends against the regional northwards ice flow, fan-shaped deposits at the northern terminus of some eskers, and a kame terrace on the southern slopes of the Sperrin Mountains. To the SW, the esker system in the Fintona Hills likely forms a meltwater routeway with the Evishanoran Esker that was active during later stages of deglaciation (Knight, 2019). We define three distinct esker sections based on variations in esker planform; the northern sector of the esker is composed of a predominantly simple system of single ridges, the central sector is dominated by a complex, arborescent ridge network distributed around a hill (~100m relief), and the southern sector comprises a complex, anabranching system of multiple subparallel ridges (Figs. 3, 4).

In the northern sector of the esker system (Fig. 4a,b), a simple planform dominates, consisting of nine consecutive ridges, with a total length of ~9 km (Table 2). The esker system trends uphill towards the NE, with ridges orientated along a uniform, broad valley bottom. However, the eskers in this sector are morphologically complex. Some consecutive ridges are offset, while others terminate in fan-shaped deposits at their northern end, or exhibit enlargements in the esker profile (Fig. 4b; Table 2). These ridges display considerable variability in size; ranging from 25 to 80 m in width and from 5 to 15 m in relief. We identify a series of six small moraine ridges across this sector, which record former ice margin



standstills. Three of the four esker enlargements and fan-shaped deposits are observed coincident with moraines.

Further SW (central sector), the esker transitions into a complex, arborescent system of short ridges (~0.3 km long) with more subdued relief (~6 m). This coincides with a change to greater variability in relief in the surrounding topography (183 – 296 m a.s.l.) and a broadly downhill trend towards the NE. The southern end of the esker is split around a hill, with the western limb trending S-N before turning W-E, where it is cross-cut by the eastern limb, which trends N-S (Figs. 2a, 4c). The esker ridges within this sector display a simple morphology, with an enlargement only observed on a single ridge. We mapped a single moraine within this esker sector, which coincided with the esker enlargement.

The southern sector consists of multiple, subparallel ridges along a slope, which broadly trends downhill to the NE. While considerable variation in relief is observed due to the undulating terrain, cross-cutting relationships are absent within this sector, although ridges are observed to bifurcate (Fig. 4d). A single small esker enlargement is observed within this sector and a small moraine is present at the eastern end of the system.

Complex geological faulting is observed across the study region (Fig. 2). Esker ridges commonly occur near faults, while some also change orientation to follow faultlines (GSNI, 2016) (Fig. 2). This is illustrated by the large fault system towards the S of the region, which trends ENE-WSW; a high concentration of esker ridges within the southern sector of the esker display a spatial correspondence to the fault and associated valley (Fig. 4d). This includes coincidence of individual ridges in the central sector of the Evishanoran Esker with faults, where the main esker trends NE-SW (Fig. 2c). Further examples of correspondence between geological faults and eskers are not limited to the Evishanoran Esker: to the west a small series of eskers change orientation to follow a fault which trends NW-SE, highlighted in Figure 2c. These changes occur three times over the ~ 5 km length of this esker.

## 4.2 Esker Internal Architecture

### 4.2.1 Radar facies (RF) description and interpretation

The GPR radar facies from both shielded 160MHz and unshielded 100MHz Rough Terrain antennas were found to be broadly comparable (see below) and are outlined in Table 1. In this section we describe facies characteristics in detail and interpret the depositional environments.

#### 4.2.1 RF1 – Coarse, poorly-bedded deposits

RF1 often constitutes the core of the esker ridge, forming a tabular unit (up to 10 m thick) of discontinuous, chaotic reflectors subparallel to the bed slope. The lower portion of RF1 often contains hyperbola-generating point reflections. This unit is conformably overlain by RF2 or RF3, or truncated by RF4 (Table 1).

Chaotic facies have been widely attributed to coarse, poorly-sorted deposits (Burke et al., 2008; Pellicer and Gibson, 2011; Franke *et al.*, 2015; Livingstone et al., 2016; Perkins et al., 2016). This is supported by sediment exposures through RF1, which comprise a variety of massive, coarse, gravelly or diamictic

deposits interpreted to have formed by the rapid deposition of hyperconcentrated flows (Fig. 5c; 5d) (Saunderson, 1977; Gorrell and Shaw, 1991; Pellicer and Gibson, 2011; Pellicer et al., 2012; Livingstone et al., 2016; Lang *et al.*, 2017). Previous studies consider point reflections to represent out-of-plane boulder clusters and a coarsening of material within the ridge (Burke, 2010; Burke et al., 2012). Out of plane reflections (sideswipes and hyperbola) are observed to be artefacts of upstanding surface objects such as trees, poles and metal farm gates (Neal, 2004). These are most notable on data from the 100MHz unshielded antenna, and thus are disregarded in our interpretations.

#### 4.2.2 RF2 – Horizontally-bedded sands

RF2 generally forms tabular units (~5 m thick) of continuous, subhorizontal reflectors (up to 30 m long) that form parallel to the bed slope (<5° dip from horizontal). It typically forms a central unit in the esker profile, regularly underlain by RF1 and overlain by RF3.

Previous studies have attributed similar patterns of subhorizontal reflectors to the vertical accretion of finer material (Perkins et al., 2016). This interpretation is consistent with sediment exposures through RF2 (Fig. 5a), which reveal horizontally-bedded sands and gravels, likely deposited in a lower flow energy environment than RF1 (Banerjee and McDonald, 1975; Burke et al., 2012).

#### 4.2.3 RF3 – Delta foresets composed of sands and gravelly sand

RF3 forms laterally constrained, wedge-shaped units (2 – 5 m thick) which unconformably overlie the older esker deposits (Table 1). They comprise a series of onlapping, low-angle (4° - 15° from horizontal), N to NE dipping reflections. RF3 is always the topmost unit where identified and therefore represents the final stage of esker building.

We interpret the dipping reflectors as foreset beds deposited during lower energy flow conditions compared to RF1 (Fiore et al., 2002; Burke et al., 2008, 2010). Foreset-backset macroforms in eskers are indicative of deposition in a subglacial conduit widening during high-energy flows (Burke *et al.*, 2010). As we do not observe any backsets associated with the foreset deposits, deposition is likely not within a subglacial conduit widening. A sediment exposure located NE of a radar survey within a ridge dominated by RF3 (Fig. 9) documents a <1 m thick unit of gravelly-sand, cross-stratified and downflow-dipping deposits (Fig. 5b). These foreset deposits are interpreted to have formed due to a change in hydraulic conditions related to flow expansion (Fiore *et al.*, 2002; Winsemann *et al.*, 2007). We interpret these deposits as either delta foresets deposited as water flowed from a subglacial conduit into a proglacial lake, in some places forming shallow-water mouth-bars (Winsemann *et al.*, 2009; 2018; Lang *et al.*, 2017), or subaqueous fan deposits (Winsemann *et al.*, 2009).

#### 4.2.4 RF4 – Concave, erosional trough-fills

RF4 is defined by strong, concave-upwards bounding reflectors and subhorizontal to concave internal reflectors (Table 1). The bounding reflectors vary in angle, with the units ranging from narrow, steep-sided basins to broader infills, which may extend for up to 60 m along the esker surface and reach thicknesses of up to 10 m. RF4 truncates underlying facies, displaying an erosional, lower bounding

surface. Most frequently, RF4 is located near the surface of the esker, but in places is conformably overlain by RF3. RF4 is interpreted as erosional troughs, formed during the late-stages of esker genesis as water incised into the underlying sediments, and subsequently filled as flow conditions waned (Gorrell and Shaw, 1991; Sambrook-Smith *et al.*, 2006; Perkins *et al.*, 2016).

#### 4.2.5 RF5 – Post-glacial infill

Present along the flanks in cross-profile surveys of esker ridges, RF5 is separated from the main esker ridge elements by a strong bounding surface, which dips steeply away from the esker (Table 1). The interior of these units is strongly attenuated and characterised by homogenous reflections, which are broadly horizontal. RF5 is interpreted as postglacial infill of the area surrounding the esker ridge. The reflection patterns are consistent with that of peat, which is prevalent across Ireland and confirmed by observations in the field (Jol and Smith, 1991; Pellicer *et al.*, 2012).

### 4.3 Site architecture

At each site, radar profiles were divided into radar facies according to Table 1 and Section 4.2 above. Here we describe the architecture of individual esker ridges and outline the processes responsible for their formation.

#### 4.3.1 Site 1

Site 1 is a 1.6 km long, broad, round-crested esker ridge at the northern termination of the single ridge esker system (northern sector). We conducted a 0.9 km, 100 MHz radar survey along a road following the crest of the esker ridge (Fig. 6). The ridge is situated along a forest-covered valley bottom on a slope that dips towards the southwest and is significantly wider than southerly ridges within the system (up to 140 m wide and 16 m high). The esker surface displays minor undulations (<1 m over ~ 90 m).

The architecture of the esker ridge is defined by a semi-continuous bounding surface with varying elevation along the upper part of the radar profile (Fig. 6). Below this bounding surface is a core of RF1 present along the whole esker profile. The chaotic reflections suggest coarser material with a lack of structure, so are interpreted to have formed by rapid deposition during high flow velocities (Burke *et al.*, 2010; Pellicer and Gibson, 2011; Franke *et al.*, 2015; Livingstone *et al.*, 2016). At around 500 m along the profile, side-swipes are observed, likely relating to signal scattering from surface obstacles (Cassidy and Jol, 2009). No lower bounding surface is observed for this unit, but a maximum thickness of 15 m is present at ~ 600 m. Towards the esker surface, the semi-continuous bounding surface defines units of RF4 from 250 m onwards. The concave trough fills (RF4) vary in size, up to ~ 6 m deep and ~ 80 m wide. At multiple locations the contact with RF4 and underlying reflectors is erosional (Fig. 6). The reflectors observed in these concave infills are less chaotic, which we interpret to have formed as erosional troughs infilled by finer sediment as flow energy waned (Sambrook-Smith *et al.*, 2006; Franke *et al.*, 2015; Table 1). Trough-fill features observed in eskers have previously been interpreted to occur when thermomechanical excavation is outweighed by creep closure, leading to increased flow velocities and the erosion of underlying sediments (Perkins *et al.*, 2016).

#### 4.3.2 Site 2

Fig. 7 shows a 0.6 km, 160 MHz radar profile taken along the crest of a 1.9 km long, round-crested ridge, near the southern end of the simple esker system (northern sector). Fig. 8 displays a cross-profile (including a short long-profile section of the crestline), taken from just over halfway along the ridge. The topographic context of the system is largely uniform, with the ridge trending up a reverse bed slope along the valley floor. The ridge morphology varies along its length. Undulations (up to 2 m high) are observed to be associated with esker widening, and the ridge generally becomes smaller towards the north (downflow), terminating in a fan-shaped deposit.

Two strong, horizontal bounding reflectors divide the ridge into three architectural units. These bounding surfaces are discordant with the undulating esker surface. The lowest bounding surface is observed at ~224 m elevation, with the underlying unit comprising a core of RF1 (present along the length of the profile). Variations in thickness (~1 - 4 m) are observed, although no clear esker base is identified. Between 0 - 10 m distance, a single unit of RF4 is present, cutting into RF1 with a depth of ~1 m. This lower radar element relates to the initial stages of esker formation, and indicates high flow energy and deposition of coarse material (Pellicer and Gibson, 2011; Livingstone *et al.*, 2016). Above the bounding surface at ~224m elevation, the radar facies of the central unit varies spatially. Chaotic reflections (RF1) dominate the upflow section from 400 – 550 m distance. Moving downflow, these reflections become more continuous and in places exhibit a downflow dip (RF3; ~ 250m distance). The change to more continuous reflectors indicates the deposition of better sorted material, perhaps due to lower energy flow conditions. Above the upper bounding surface (225 m elevation), a ~2 m thick, tabular unit of RF3 is continuous between 0 – 200 m distance, but absent from 200 – 400 m distance. The presence of coherent downflow dipping reflectors (RF3) indicates a switch to lower flow energy conditions in a progradational depositional environment. Within Figure 8, RF3 has a convex-up, lenticular reflector pattern. This may represent laterally and vertically stacked, shallow-water delta mouth-bar lobes deposited at the ice sheet margin where water from the subglacial conduit enters a glacial lake (Winsemann *et al.*, 2018). However, we are cautious not to overinterpret this portion of the radar survey due to the non-linear survey route. This unit unconformably overlies the esker core and does not extend over the esker flanks, coinciding with an increase in esker height. This suggests that deposition was constrained by ice walls (Fig. 8). Foreset-backset macroforms have been associated with dynamic subglacial conduit enlargements during high flow energy conditions (Fiore *et al.*, 2002; Burke *et al.*, 2010). The absence of backset deposits within this esker suggests another mechanism was responsible for the change to progradational deposition.

Between 400 - 500 m distance, subhorizontal to chaotic reflections (RF1 and RF2) are observed along the esker surface, coincident with an undulation and widening of the esker ridge. Overall, esker architecture records a transition from hyperconcentrated flows during the initial stages, to lower energy flow conditions and the deposition of delta foresets at the ice sheet margin. In cross-profile, up to 8 m

of post-glacial peat deposition (RF5) is documented on the esker flanks. This may result in less than 50% of the true esker height being observable at the surface (Jol and Smith, 1991; Pellicer *et al.*, 2012).

#### 4.3.3 Site 3

Figure 9 presents a 0.2 km, 160 MHz radar profile along the crest of a 0.8 km long round-topped esker ridge, within the complex multi-ridge system (central sector). The ridge is situated in an area of steep, hilly topography. At ~300 m along the esker morphology develops from a narrow ridge (~50 m wide) into a broad, fan-shaped enlargement which is ~130 m wide and ~250 m long, before the ridge terminates in a narrower section (~50 m wide) that is ~200 m long in an open topographic basin that drains to the northwest. The radar profile starts on the summit of a hill at the beginning of the enlargement and then follows the esker crest downslope (Fig 9). Three other ridges are located adjacent to the studied esker, terminating in the same basin. A gravel pit is located at the terminus of the ridge, consisting of a series of sand and gravel foreset units which dip to the northeast (Fig. 5b).

Within the lowest radar unit, between 0 – 40 m distance, the sequence is dominated by at least 3 m of coherent horizontal reflections (RF2) indicating vertical accretion of fine material (Burke *et al.*, 2012). Poor radar penetration prevents the identification of the lower bounding surface of this unit. From 120 – 170 m along flow, a unit up to 7 m thick, composed of more discontinuous reflections (RF1 and RF2), represents a lateral transition to coarser material lacking structure, interpreted to be deposited subglacially under higher flow energy (Pellicer and Gibson, 2011; Franke *et al.*, 2015; Livingstone *et al.*, 2016). The upper section of the radar profiles is dominated by continuous, downflow-dipping parallel reflectors which are convex-up lenticular perpendicular to flow. These units are typically quite thin (up to ~2m) with low dip angles. From 0 – 140 m, there are two units of RF3 along the surface, but 140 m onwards is characterised by a single unit of RF3 along the surface. These upper units likely represent a series of delta foresets and cross-stratified sands and gravels, deposited during lower energy flow conditions in a progradational environment (Franke *et al.*, 2015). The thin beds and low dip angle suggest deposition within a shallow water environment (Winsemann *et al.*, 2018). We interpret this sequence of foresets, composed of cross-stratified sands and gravels, as shallow-water delta foresets deposited on top of an esker, as meltwater exits the subglacial conduit at the ice sheet margin (Winsemann *et al.*, 2007). The transition to a broader, fan-shaped morphology of the esker enlargement associated with RF3 supports the interpretation that the delta foresets are superimposed on a core of esker material that was deposited subglacially (Fig. 9).

#### 4.3.4 Site 4

Figure 10 shows a 0.18 km long, 160 MHz radar profile along part of the crest of a 0.75 km long round-crested esker within the complex, multi-ridge to anabranching esker system (southern sector). The esker system is situated in an area of complex, hilly topography. The general esker trend is subparallel to a fault-controlled valley, with ridges situated in and around it (Fig. 5d).

A single bounding surface is semi-continuous along the radar profile, present from 0 – 70 m distance, at an elevation of ~ 233 m (Fig. 10). Below this bounding surface, a ~2 m thick core unit of chaotic reflections (RF1) is present in sections of the radar profile where penetration was deep enough. These chaotic reflections suggest the presence of coarse material deposited under high energy flow conditions (Pellicer and Gibson, 2011; Livingstone *et al.*, 2016). Above the bounding surface, the radar units (~4 m thick) comprise more continuous reflections which are either subhorizontal or downflow dipping (RF2 and RF3). This represents an increase in structure as finer material was deposited during lower energy flow conditions (Franke *et al.*, 2015). The upflow section (0 - 80 m distance) is dominated by RF1 and RF2, while the downflow section (80 m distance onwards) consists of more coherent units of RF3. This transition to fine-grained foresets (RF3) coincides with a change to a downslope trend.

## 5.0 Discussion

The following section seeks to further our understanding of esker formation based on the sedimentary architecture of a morphologically diverse esker system. First, the broad-scale architecture is considered in order to develop a depositional model of esker formation. Second, local controls on esker formation and morphology are discussed. Finally, we use our findings to reconstruct the ice sheet retreat pattern and retreat rate for the Omagh Basin region.

### 5.1 Esker formation

#### 5.1.1 A time-transgressive model of esker deposition

The Evishanoran Esker has a broadly homogeneous large-scale sedimentary architecture, despite changes in esker morphology and topographic context (Figs. 6-10). GPR surveys reveal two main styles of deposition during esker formation. Initial esker growth involved deposition of coarse gravel or diamict from subglacial hyperconcentrated flows, which may have occurred in a somewhat synchronous manner (Saunderson, 1977; Gorrell and Shaw, 1991; Pellicer and Gibson, 2011). Offset ridge relationships and eskers terminating in subaqueous fans or deltas in the northern sector suggest that this deposition likely extended for a maximum of a few kilometres up-ice, rather than tens of kilometres (Fig. 4b). Later stages of esker growth coincide with a transition to well-sorted, deposits as flow energy waned (Franke *et al.*, 2015). The sedimentary structures document a variety of hydrological processes during the final stages of formation (RF2, RF3 and RF4), in contrast to the simple earlier event dominated by hyperconcentrated flows (RF1).

As meltwater approaches the ice sheet margin, subglacial conduits experience reduced creep closure (reaching zero at the ice margin: Rothlisberger, 1972). Despite this, thermomechanical excavation continues to enlarge the subglacial conduit, meaning that the subglacial conduit grows towards the ice sheet margin (Drews *et al.*, 2017). This expansion of the subglacial conduit is expected to cause a progressive reduction in flow energy and carrying capacity (Hewitt and Creyts, 2019), resulting in increased sedimentation rates (Beaud *et al.*, 2018) and the deposition of well-sorted, finer material. This results in an enlargement of the esker profile at or near to former ice margin standstills (Fig. 11a). Flow

expansion due to conduit enlargement and subglacial meltwater drainage into the proglacial lake caused a fall in flow energy and the formation of deltas/outwash fans (Winsemann *et al.*, 2007). In this situation, the observed vertical upwards-sorting sequence is associated with decreasing flow energy as deposition occurs progressively closer to the ice sheet margin during retreat (Walther, 1894).

Esker size, and the thickness of stratigraphic units, is dependent on the duration and rate of deposition. As we described, the deposition rate is likely linked to the proximity of a location to the ice sheet margin, as well as rates of sediment supply. The duration of deposition is related to the rate of ice sheet margin retreat. Rapid margin retreat will reduce the time available for deposition, while a standstill will result in enhanced deposition at and near the ice sheet margin. Therefore, we suggest that enlargements in the esker profile could indicate former ice margin positions. For a stable ice sheet margin position, we would expect a simple esker profile which grows in size towards its terminus. However, variations in the retreat rate during deglaciation will lead to the superimposition of later esker deposits during time-transgressive esker formation (Fig. 11b). We suggest the observed esker enlargements are a form of esker bead deposited time-transgressively at the ice sheet margin (e.g. Livingstone *et al.*, 2020), and superimposed on the core of subglacially deposited coarser material (Fig. 7, 9 and 11).

Enlargements in eskers or outwash fans/deltas are commonly observed across the Evishanoran Esker. We suggest these enlargements can be used to reconstruct the relative rate of ice sheet margin retreat and former ice margin positions. We favour formation of enlargements at the ice sheet margin, over the possibility of formation within subglacial conduits, as we do not observe a backset-foreset macroform diagnostic of this formation (Burke *et al.*, 2015). Caution must be taken when using these to reconstruct the retreat rate, as variations in sediment supply may also influence the development of these enlargements. But, the common co-occurrence of esker enlargements with topographic pinning points (Fig. 4a) or moraines (Fig. 4b) supports an ice marginal origin.

Morphogenetic relationships have been proposed for eskers on the southern Fraser Plateau, British Columbia (Burke *et al.*, 2015; Perkins *et al.*, 2016), while esker complexity has been related to meltwater flow conditions and sediment supply in Svalbard and Iceland (Storarr *et al.*, 2015, 2020). In central Northern Ireland, the relationship between esker morphology and the depositional processes is less clear. At the local scale, undulations and enlargements of the esker profile appear to relate to a time-transgressive depositional model during ice sheet retreat. An esker core is formed by synchronous subglacial deposition, while enlargements are formed by the time-transgressive deposition of sediment at or near to the ice sheet margin (Fig. 11).

#### 5.1.2 Local controls

The morphology of eskers is influenced by the overall drainage characteristics during formation (Burke *et al.*, 2015; Storarr *et al.*, 2015), as well as local factors (Clark and Walder, 1994; Storarr *et al.*, 2014a; Knight, 2019). Beneath the Laurentide Ice Sheet, complex eskers and drainage routeways are more common in areas of greater topographic variability (Storarr *et al.*, 2014a; Lewington *et al.*, 2020). In

the Evishanoran Esker, a similar relationship between complex esker morphology and topography is observed. At the large-scale, the complex southern and central esker planforms are associated with a topographic context dominated by high variations in relief, while the simpler northern sector is located on the bottom of a broad valley floor. The distribution of eskers in the central sector clearly illustrates this topographic influence, as eskers are deflected around the ~100m hill (Fig. 4c). We propose that esker complexity in central Northern Ireland is largely controlled by the topographic variability. Undulating topography may cause the subglacial conduit to fragment around obstacles or migrate as ice thinned (Wright *et al.*, 2008; Storrar *et al.*, 2014b).

The complexity of esker systems in areas of high topographic variability reflects a combination of spatial and temporal changes in the subglacial drainage network. Within the central sector of the Evishanoran Esker, cross-cutting ridges suggest that the drainage system migrated during deglaciation to create the complex esker network (Fig. 4c). In contrast, the anabranching nature of the southern sector, with no cross-cutting relationships may instead represent a drainage network which is fragmented by the complex topography (Fig. 4d). This is supported by the association with a series of meltwater channels cut into, and ascending, the hill to the south of this sector (Fig. 2b), which may have been active at similar times. Pressurised meltwater eroded the meltwater channels on the southern slopes of the hill. Reductions in pressure on the downslope trend then led to the deposition of the esker system (Livingstone *et al.*, 2016). It is also possible that increased deposition on the downslope trend may have led to channel clogging and avulsion (Storrar *et al.*, 2015).

Substrate characteristics have been hypothesised to influence the formation and distribution of eskers. For example, eskers are more common on resistant bedrock (Clark and Walder, 1994). Esker morphology in north-central Ireland is controlled by a variety of substrate factors, including the influence of pre-existing glacial features (Knight, 2019). The transition from sandstone and limestone in the south to the variably metamorphosed crystalline granites and gabbros in the north does not appear to influence esker distribution in the region south of the Sperrin Mountains. This is despite the fundamental differences in bedrock structure at the crystal scale. However, a high level of spatial correspondence between eskers and geological faults is observed (Fig. 2). This correspondence includes eskers in the southern sector running sub-parallel to a large fault-controlled valley, and pronounced changes in the orientation of eskers to trend along faults (Fig. 2). The valley orientation also likely plays a role in controlling the esker distribution. However, esker distribution appears to be fault-controlled across central Northern Ireland, including in locations where there is no clear topographic control. Enhanced groundwater flow along zones of higher transmissivity (e.g. faults) may influence the distribution of the subglacial drainage system (Boulton *et al.*, 2007a; 2007b; 2009).

The morphometry of eskers may relate to a combination of sediment and meltwater supply (Shreve, 1985; Storrar *et al.*, 2015), but caution must be taken when solely using geomorphological observations to investigate the hydrological system of a palaeo-ice sheet. Radar surveys revealed substantial post-



glacial peat infilling around eskers, reducing their relative relief in the northern sector. The relative relief of one esker is 5 m, but with up to 6 m of esker deposits hidden below the surface (Fig. 8). Extensive peat deposits, up to 5.5 m thick, have been documented in the Irish Midlands (Pellicer and Gibson, 2011; Pellicer *et al.*, 2012), which must be taken into consideration when using esker dimensions to gain an insight into glacial history.

## 5.2 Implications for deglaciation of Northern Ireland

Three main ice dispersal centres operated during the deglaciation of the north of Ireland. This includes an upland ice dispersal centre in the Donegal Mountains, and lowland ice domes in the Lough Neagh and Omagh basins (Knight, 1997; Knight and McCabe, 1997; McCarron, 2013). Across this region, meltwater landforms and small moraines record the final retreat pattern of the Irish Ice Sheet. Here we describe the broader retreat patterns of the Irish Ice Sheet, before using the Evishanoran Esker to describe the retreat rate of the Omagh Basin ice.

The Donegal Mountains, Lough Neagh and Omagh ice domes were coalescent at the start of deglaciation, indicated by subglacial bedform patterns (Fig. 2a), but became isolated ice domes following ice sheet thinning (Fig. 2a and 2b). Eskers oriented radially around the Lough Neagh basin record the final pattern of retreat. Lough Neagh ice separated from the Lough Erne/Omagh Basin Ice Dome along an approximately N-S axis located to the south of the eastern Sperrin Mountains (Fig. 2a). In the west, the Lough Erne Ice Dome separated from ice sourced from the Donegal and Sligo Mountains sometime between 15-16ka, according to the isochrons of Wilson *et al.* (2019). Lateral meltwater channels record the downwasting of ice flowing from Sligo and Donegal into the Lough Erne Basin, indicating when summits became ice-free and the separation of these ice dispersal centres (Fig. 2b). The position of these channels suggests that Donegal ice persisted long enough to flow into a mostly deglaciated Lough Erne Basin (Fig. 2b). This is consistent with dating evidence indicating that the Donegal Mountains held the final remnants of the British-Irish Ice Sheet in Ireland (Wilson *et al.*, 2019). The relative retreat rate and former ice margin standstills can be identified from the morphology of the Evishanoran Esker and associated landforms. The initial southwards ice margin retreat from the Sperrin Mountains was quite slow across the northern esker sector. We identify at least four former ice margin standstills over the 9.3 km this sector spans, from evidence of five small moraines, two esker enlargements, three delta/outwash fan deposits and sedimentological information (Fig. 2b,c). These former standstill locations are mostly located at topographic pinning points. The retreat rate was more rapid across the central sector. A single moraine and fan-shaped deposit at the northern end of this sector suggest only one standstill across the 7.4 km sector length. The retreat rate across the southern sector may have slowed slightly, as the retreat direction became oriented towards the SW. Geomorphological evidence suggests one or two possible standstills over a distance of 6.5 km. A small moraine at the north-eastern side of the sector suggests a standstill at the start of esker formation in this sector, where a hill (~150m relative relief) may have acted as a pinning point. A small enlargement associated with

foreset deposits may have formed under a short-lived standstill in the centre of this sector (Fig. 10). However, the retreat was likely more rapid than in the northern sector due to the relative lack of geomorphological evidence. Continued retreat to the SW of our study area led to the formation of eskers and meltwater channels throughout the Lough Erne Basin and Fintona Hills (Knight, 2003; 2019).

## **6.0 Conclusions**

The Evishanoran Esker was deposited time-transgressively in a subglacial, closed conduit or at the ice sheet margin and records the final stages of ice retreat in this region from the Sperrin Mountains to the south. Esker distribution is a result of the dynamic evolution of the subglacial hydrological system, and does not record an extensive drainage network. Based on our observations, we present a series of key points regarding the deglacial history and broader implications for esker formation:

1. The Evishanoran Esker was formed by two main styles of deposition that occurred repeatedly during deglaciation. An initial event of hyperconcentrated flows within the subglacial conduit deposited the poorly sorted, coarse sediment that forms the esker core. This subglacial deposition likely occurred in a semi-synchronous manner. This was followed by the deposition of delta foresets composed of well-sorted material, superimposed on the subglacially deposited esker core. These delta foresets were deposited time-transgressively at or near the ice sheet margin due to flow expansion as subglacial meltwater entered a proglacial lake. Esker enlargements occur where these time-transgressive delta deposits are observed, and likely indicate former ice margin positions.
2. The internal architecture of eskers is broadly homogenous across all sectors, suggesting that hydrological conditions are largely comparable. Variations in esker morphology cannot solely be attributed to variations in drainage characteristics. Instead, we suggest local topographic conditions influence esker complexity.
3. Using evidence for former ice margin standstills we reconstruct the variations in the retreat rate across the Evishanoran Esker. Ice margin retreat across the northern sector was slow, with retreat rate increasing during margin retreat across the central and southern sectors.
4. Geologic and topographic settings control esker distribution and formation. The close association between the orientation and distribution of eskers and faults suggest that underlying geological structural weaknesses act as a zone of high meltwater transmissivity. The reconstruction of ice dynamics from meltwater features must also consider the influence of local factors on distribution.
5. Post-depositional processes can have a significant influence on esker geomorphology. Post-glacial fluvial erosion has previously been invoked to explain the fragmentation of some esker systems. We identify significant post-glacial peat infilling which masks esker dimensions and poses a problem for esker studies that rely solely on remote sensing morphometric analysis.

**Acknowledgements:**

We thank Mike Langton of GuideLineGeo (MALA) for the loan of radar equipment and advice. Digital resources were made available under MOU205, courtesy of Land and Property Services, Northern Ireland, supplied to Queen's University, Belfast. This study would also not be possible without the generous access to land granted by multiple landowners in Northern Ireland. We kindly thank two anonymous reviewers for their comments on this manuscript.

**Funding sources:**

This research did not receive any specific grant from funding agencies in the public, commercial, or not-for-profit sectors.

**References:**

- Alley, R.B., Blankenship, D.D., Bentley, C.R. and Rooney, S.T. (1986) Deformation of till beneath ice stream B, West Antarctica. *Nature*, 322, 57-59.
- Aylsworth, J.M. and Shilts, W.W. (1989) Bedforms of the Keewatin ice sheet, Canada. *Sedimentary Geology*, 62(2-4): 407-428
- Banerjee, I. and McDonald, B.C. (1975) Nature of esker sedimentation, in Jopling, A. V., and McDonald, B. C., eds., *Glaciofluvial and glaciolacustrine sedimentation*: Society of Economic Paleontologists and Mineralogists Special Publication No. 23: 132-154.
- Bartholomew, I., Nienow, P., Mair, D., Hubbard, A., King, M.A. and Sole, A. (2010). Seasonal evolution of subglacial drainage and acceleration in a Greenland outlet glacier. *Nature Geoscience*, 3(6), 408-411.
- Beaud, F., Flowers, G.E. and Venditti, J.G. (2018) Modeling Sediment Transport in Ice-Walled Subglacial Channels and Its Implications for Esker Formation and Proglacial Sediment Yields. *Journal of Geophysical Research: Earth Surface*, 123(12): 3206-3227
- Bell, R.E., Studinger, M., Shuman, C.A., Fahnestock, M.A. and Joughin, I. (2007). Large subglacial lakes in East Antarctica at the onset of fast-flowing ice streams. *Nature*, 445(7130), 904-907.
- Boulton, G.S., Hagdorn, M., Maillot, P.B. and Zatsepin, S. (2009) Drainage beneath ice sheets: groundwater–channel coupling, and the origin of esker systems from former ice sheets. *Quaternary Science Reviews*, 28(7-8), 621-638

- 643 Boulton, G.S., Lunn, R., Vidstrand, P. and Zatsepin, S. (2007b) Subglacial drainage by  
644 groundwater–channel coupling, and the origin of esker systems: part II—theory and  
645 simulation of a modern system. *Quaternary Science Reviews*, 26(7-8), 1091-1105
- 646 Boulton, G.S., Lunn, R., Vidstrand, P. and Zatsepin, S., (2007a) Subglacial drainage by  
647 groundwater-channel coupling, and the origin of esker systems: part 1—glaciological  
648 observations. *Quaternary Science Reviews*, 26(7-8), 1067-1090
- 649 Bradwell, T., Stoker, M.S., Golledge, N.R., Wilson, C.K., Merritt, J.W., Long, D., Everest, J.D.,  
650 Hestvik, O.B., Stevenson, A.G., Hubbard, A.L. and Finlayson, A.G. (2008) The northern  
651 sector of the last British Ice Sheet: maximum extent and demise. *Earth-Science*  
652 *Reviews*, 88(3-4): 207-226
- 653 Brennand, T. A. (1994). Macroforms, large bedforms and rhythmic sedimentary sequences in  
654 subglacial eskers, south-central Ontario: implications for esker genesis and meltwater  
655 regime. *Sedimentary Geology*, 91(1–4), 9–55. [https://doi.org/10.1016/0037-0738\(94\)90122-](https://doi.org/10.1016/0037-0738(94)90122-8)  
656 [8](https://doi.org/10.1016/0037-0738(94)90122-8)
- 657 Brennand, T.A. (2000) Deglacial meltwater drainage and glaciodynamics: inferences from  
658 Laurentide eskers, Canada. *Geomorphology*, 32(3-4): 263-293
- 659 Budd, W.F., Keage, P.L. and Blundy, N.A (1979). Empirical studies of ice sliding. *Journal of*  
660 *Glaciology*, 23, 157-170.
- 661 Burke, M. J., Brennand, T. A., & Sjogren, D. B. (2015). The role of sediment supply in esker  
662 formation and ice tunnel evolution. *Quaternary Science Reviews*, 115, 50–77.  
663 <https://doi.org/10.1016/j.quascirev.2015.02.017>
- 664 Burke, M. J., Woodward, J., Russell, A. J., Fleisher, P. J., & Bailey, P. K. (2008). Controls on the  
665 sedimentary architecture of a single event englacial esker: Skeiðarárjökull, Iceland.  
666 *Quaternary Science Reviews*, 27(19–20): 1829–1847.  
667 <https://doi.org/10.1016/j.quascirev.2008.06.012>
- 668 Burke, M. J., Woodward, J., Russell, A. J., Fleisher, P. J., & Bailey, P. K. (2010). The sedimentary  
669 architecture of outburst flood eskers: A comparison of ground-penetrating radar data from  
670 Bering Glacier, Alaska and Skeiðarárjökull, Iceland. *Bulletin of the Geological Society of*  
671 *America*, 122(9–10): 1637–1645. <https://doi.org/10.1130/B30008.1>

672 Burke, M.J., Brennand, T.A. and Perkins, A.J. (2012) Transient subglacial hydrology of a thin ice  
673 sheet: insights from the Chasm esker, British Columbia, Canada. *Quaternary Science*  
674 *Reviews*, 58: 30-55.

675 Callard, S.L., Cofaigh, C.Ó., Benetti, S., Chiverrell, R.C., Van Landeghem, K.J., Saher, M.H.,  
676 Livingstone, S.J., Clark, C.D., Small, D., Fabel, D. and Moreton, S.G. (2020) Oscillating  
677 retreat of the last British-Irish Ice Sheet on the continental shelf offshore Galway Bay,  
678 western Ireland. *Marine Geology*, 420: 106087.

679 Cassidy, N.J. and Jol, H.M. (2009) Ground penetrating radar data processing, modelling and  
680 analysis. *Ground penetrating radar: theory and applications*: 141-176

681 Charlesworth, J.K. (1926) The Evishnoran “Esker”, Tyrone. *Geological Magazine*, 63(5), 223-225.  
682 doi:10.1017/S0016756800084156

683 Charlesworth, J.K. (1924). The glacial geology of the north-west of Ireland. *Proceedings of the*  
684 *Royal Irish Academy*, 36b: 174-314

685 Chew, D.M., Flowerdew, M.J., Page, L.M., Crowley, Q.G., Daly, J.S., Cooper, M. and Whitehouse,  
686 M.J. (2008) The tectonothermal evolution and provenance of the Tyrone Central Inlier,  
687 Ireland: Grampian imbrication of an outboard Laurentian microcontinent?. *Journal of the*  
688 *Geological Society*, 165(3): 675-685

689 Chiverrell, R.C., Thomas, G.S.P., Burke, M., Medialdea, A., Smedley, R., Bateman, M., Clark, C.,  
690 Duller, G.A., Fabel, D., Jenkins, G. and Ou, X. (2020) The evolution of the terrestrial-  
691 terminating Irish Sea glacier during the last glaciation. *Journal of Quaternary Science*,  
692 doi:10.1002/jqs.3229

693 Clark, C.D. and Meehan, R.T. (2001) Subglacial bedform geomorphology of the Irish Ice Sheet  
694 reveals major configuration changes during growth and decay. *Journal of Quaternary*  
695 *Science: Published for the Quaternary Research Association*, 16(5): 483-496

696 Clark, C.D., Ely, J.C., Greenwood, S.L., Hughes, A.L., Meehan, R., Barr, I.D., Bateman, M.D.,  
697 Bradwell, T., Doole, J., Evans, D.J. and Jordan, C.J. (2018) BRITICE Glacial Map, version  
698 2: a map and GIS database of glacial landforms of the last British–Irish Ice  
699 Sheet. *Boreas*, 47(1): 11

700 Clark, C.D., Hughes, A.L., Greenwood, S.L., Jordan, C. and Sejrup, H.P. (2012) Pattern and timing  
701 of retreat of the last British-Irish Ice Sheet. *Quaternary Science Reviews*, 44: 112-146

702 Clark, P. U., & Walder, J. S. (1994). Subglacial drainage, eskers, and deforming beds beneath the  
703 Laurentide and Eurasian ice sheets. *Geological Society of America Bulletin*, 106(2), 304–  
704 314. [https://doi.org/10.1130/0016-7606\(1994\)106<0304:SDEADB>2.3.CO;2](https://doi.org/10.1130/0016-7606(1994)106<0304:SDEADB>2.3.CO;2)

705 Colhoun, A. (1971) The glacial stratigraphy of the Sperrin Mountains and its relation to the glacial  
706 stratigraphy of north-west Ireland. *Proceedings of the Royal Irish Academy* 71B: 37–52

707 Colhoun, E.A. (1970). On the nature of the glaciations and final deglaciation of the Sperrin  
708 Mountains and adjacent areas in the north of Ireland. *Irish Geography*, 6(2), 162-185.

709 Cummings, D.I., Kjarsgaard, B.A., Russell, H.A. and Sharpe, D.R. (2011) Eskers as mineral  
710 exploration tools. *Earth-science reviews*, 109(1-2): 32-43

711 Dardis, G.F. (1986) Late Pleistocene glacial lakes in south-central Ulster, Northern Ireland. *Irish*  
712 *journal of earth sciences*: 133-144

713 Davison, B.J., Sole, A.J., Livingstone, S.J., Cowton, T.R. and Nienow, P.W. (2019) The influence of  
714 hydrology on the dynamics of land-terminating sectors of the Greenland Ice Sheet. *Frontiers*  
715 *in Earth Science*, 7.

716 Delaney, C. (2001a) Esker formation and the nature of deglaciation: the Ballymahon esker, Central  
717 Ireland. *North West Geography*, 1(2): 23-33

718 Delaney, C. (2001b) Morphology and sedimentology of the Rooskagh esker, Co. Roscommon. *Irish*  
719 *Journal of Earth Sciences*: 5-22

720 Delaney, C. (2002) Sedimentology of a glaciofluvial landsystem, Lough Ree area, Central Ireland:  
721 implications for ice margin characteristics during Devensian deglaciation. *Sedimentary*  
722 *Geology*, 149(1-3): 111-126

723 Delaney, C.A., McCarron, S. and Davis, S. (2018). Irish Ice Sheet dynamics during deglaciation of  
724 the central Irish Midlands: Evidence of ice streaming and surging from airborne LiDAR.  
725 *Geomorphology*, 306, 235-253.

726 Drews, R., Pattyn, F., Hewitt, I.J., Ng, F.S.L., Berger, S., Matsuoka, K., Helm, V., Bergeot, N.,  
727 Favier, L. and Neckel, N. (2017) Actively evolving subglacial conduits and eskers initiate  
728 ice shelf channels at an Antarctic grounding line. *Nature communications*, 8: 15228

729 Dyke, A. and Prest, V. (1987) Late Wisconsinan and Holocene history of the Laurentide ice  
730 sheet. *Géographie physique et Quaternaire*, 41(2): 237-263.

- 731 Evans, D. J. A., & Benn, D. I. (2004) A practical guide to the study of glacial sediments. Edward  
732 Arnold, London.
- 733 Fiore, J., Pugin, A. and Beres, M. (2002) Sedimentological and GPR studies of subglacial deposits  
734 in the Joux Valley (Vaud, Switzerland): backset accretion in an esker followed by an erosive  
735 jökulhlaup. *Géographie physique et Quaternaire*, 56(1): 19-32
- 736 Fitzsimons, S.J. (1991) Supraglacial eskers in Antarctica. *Geomorphology*, 4(3-4): 293-299
- 737 Flint, R.F. (1930) The Origin of the Irish" Eskers". *Geographical Review*, 20(4): 615-630
- 738 Franke, D., Hornung, J. and Hinderer, M. (2015) A combined study of radar facies, lithofacies and  
739 three-dimensional architecture of an alpine alluvial fan (Illgraben fan,  
740 Switzerland). *Sedimentology*, 62(1): 57-86
- 741 Gawthorpe, R.L., Collier, R.L., Alexander, J., Bridge, J.S. and Leeder, M.R. (1993) Ground  
742 penetrating radar: application to sandbody geometry and heterogeneity studies. *Geological*  
743 *Society, London, Special Publications*, 73(1): 421-432
- 744 Geological Survey Northern Ireland (2016) Digital Geological Map of Northern Ireland – 10k. 10k  
745 geology reproduced with the permission of the Geological Survey of Northern Ireland.  
746 Crown Copyright 2018.
- 747 Gorrell, G. and Shaw, J. (1991) Deposition in an esker, bead and fan complex, Lanark, Ontario,  
748 Canada. *Sedimentary Geology*, 72(3-4): 285-314
- 749 Greenwood, S. L., & Clark, C. D. (2009a). Reconstructing the last Irish Ice Sheet 1: changing flow  
750 geometries and ice flow dynamics deciphered from the glacial landform record. *Quaternary*  
751 *Science Reviews*, 28(27–28), 3085–3100. <https://doi.org/10.1016/j.quascirev.2009.09.008>
- 752 Greenwood, S. L., & Clark, C. D. (2009b). Reconstructing the last Irish Ice Sheet 2: a  
753 geomorphologically-driven model of ice sheet growth, retreat and dynamics. *Quaternary*  
754 *Science Reviews*, 28(27–28), 3101–3123. <https://doi.org/10.1016/j.quascirev.2009.09.014>
- 755 Greenwood, S.L., Clark, C.D. and Hughes, A.L. (2007) Formalising an inversion methodology for  
756 reconstructing ice-sheet retreat patterns from meltwater channels: application to the British  
757 Ice Sheet. *Journal of Quaternary Science: Published for the Quaternary Research*  
758 *Association*, 22(6): 637-645

- 759 Greenwood, S.L., Clason, C.C., Helanow, C. and Margold, M. (2016) Theoretical, contemporary  
760 observational and palaeo-perspectives on ice sheet hydrology: processes and  
761 products. *Earth-Science Reviews*, 155: 1-27
- 762 Gregory, J.W. (1912) The relations of kames and eskers. *The Geographical Journal*, 40(2): 169-175.
- 763 Gregory, J.W. (1921) IV.—The Irish eskers. *Phil. Trans. R. Soc. Lond. B*, 210(372-381): 115-151.
- 764 Gregory, J.W. (1925) The Evishanoran Esker, 1 Tyrone. *Geological Magazine*, 62(10): 451-458.
- 765 Gregory, J.W. (1926) The Evishnoran “Esker”. *Geological Magazine*, 62(7): 336-336.  
766 doi:10.1017/S0016756800084557
- 767 Gustavson, T.C. and Boothroyd, J.C. (1987) A depositional model for outwash, sediment sources,  
768 and hydrologic characteristics, Malaspina Glacier, Alaska: A modern analog of the  
769 southeastern margin of the Laurentide Ice Sheet. *Geological Society of America*  
770 *Bulletin*, 99(2): 187-200.
- 771 Hebrand, M. and Åmark, M. (1989) Esker formation and glacier dynamics in eastern Skane and  
772 adjacent areas, southern Sweden. *Boreas*, 18(1): 67-81.
- 773 Hewitt, I.J. and Creyts, T.T. (2019) A model for the formation of eskers. *Geophysical Research*  
774 *Letters*, 46(12), pp.6673-6680.
- 775 Hinch, J. (1921) The eskers of Ireland. *The Irish Naturalist*, 30(12): 137-142
- 776 Hubbard, B. & Nienow, P. (1997) Alpine subglacial hydrology. *Quaternary Science Reviews*, 16,  
777 939-955.
- 778 Iken, A., Bindschadler, R.A. (1986) Combined measurements of subglacial water pressure and  
779 surface velocity of Findelengletscher, Switzerland: conclusions about drainage system and  
780 sliding mechanism. *Journal of Glaciology*, 32(110): 101-119.
- 781 Jol, H.M. and Smith, D.G. (1991) Ground penetrating radar of northern lacustrine deltas. *Canadian*  
782 *Journal of Earth Sciences*, 28(12): 1939-1947
- 783 Knight, J. (1997). Morphological and morphometric analysis of drumlin bedforms in the Omagh  
784 Basin, north central Ireland. *Geografiska Annaler*, 79A: 255-266.
- 785 Knight, J. (1999). Geological evidence for neotectonic activity during deglaciation of the southern  
786 Sperrin Mountains, Northern Ireland. *Journal of Quaternary Science*, 14(1): 45-57.



787 Knight, J. (2002). Bedform patterns, subglacial meltwater events, and Late Devensian ice sheet  
788 dynamics in north-central Ireland. *Global and Planetary Change*, 35(3–4): 237–253.

789 Knight, J. (2003) Geomorphic evidence for patterns of late Midlandian ice advance and retreat in the  
790 Omagh Basin. *Irish Geography*, 36(1): 1-22

791 Knight, J. (2006) Geomorphic evidence for active and inactive phases of Late Devensian ice in  
792 north-central Ireland. *Geomorphology*, 75(1-2): 4-19

793 Knight, J. (2019) The geomorphology and sedimentology of eskers in north-Central  
794 Ireland. *Sedimentary Geology*, 382: 1-24.

795 Knight, J. and McCabe, A.M. (1997) Identification and significance of ice-flow-transverse  
796 subglacial ridges (Rogen moraines) in northern central Ireland. *Journal of Quaternary*  
797 *Science*, 12(6): 519-524

798 Knight, J., Coxon, P., McCabe, A.M. and McCarron, S.G. (2004) Pleistocene glaciations in Ireland.  
799 In *Developments in Quaternary Sciences*, 2: 183 – 191. Elsevier.

800 Lang, J., Sievers, J., Loewer, M., Igel, J. and Winsemann, J. (2017) 3D architecture of cyclic-step  
801 and antidune deposits in glaciogenic subaqueous fan and delta settings: Integrating outcrop  
802 and ground-penetrating radar data. *Sedimentary Geology*, 362: 83-100

803 Lewington, E.L., Livingstone, S.J., Clark, C.D., Sole, A.J. and Storrar, R.D. (2020) A model for  
804 interaction between conduits and surrounding hydraulically connected distributed drainage  
805 based on geomorphological evidence from Keewatin, Canada. *The Cryosphere*, 14(9): 2949-  
806 2976.

807 Livingstone, S. J., Utting, D. J., Ruffell, A., Clark, C. D., Pawley, S., Atkinson, N., & Fowler, A. C.  
808 (2016). Discovery of relict subglacial lakes and their geometry and mechanism of drainage.  
809 *Nature Communications*, 7. <https://doi.org/10.1038/ncomms11767>

810 Livingstone, S.J., Lewington, E.L., Clark, C.D., Storrar, R.D., Sole, A.J., McMartin, I., Dewald, N.  
811 and Ng, F. (2020) A quasi-annual record of time-transgressive esker formation: implications  
812 for ice-sheet reconstruction and subglacial hydrology. *The Cryosphere*, 14(6): 1989-2004

813 Livingstone, S.J., Storrar, R.D., Hillier, J.K., Stokes, C.R., Clark, C.D. and Tarasov, L. (2015) An  
814 ice-sheet scale comparison of eskers with modelled subglacial drainage  
815 routes. *Geomorphology*, 246: 104-112

816 Mäkinen, J. (2003) Time-transgressive deposits of repeated depositional sequences within  
817 interlobate glaciofluvial (esker) sediments in Köyliö, SW Finland. *Sedimentology*, 50(2):  
818 327-360

819 Margold, M., Jansson, K.N., Kleman, J., Stroeven, A.P. and Clague, J.J. (2013) Retreat pattern of  
820 the Cordilleran Ice Sheet in central British Columbia at the end of the last glaciation  
821 reconstructed from glacial meltwater landforms. *Boreas*, 42(4): 830-847

822 McCarron, S. (2013) Deglaciation of the Dungiven Basin, North-West Ireland. *Irish Journal of*  
823 *Earth Sciences*, 31: 43-71

824 Miall, A.D. (1985) Architectural-element analysis: a new method of facies analysis applied to fluvial  
825 deposits. *Earth Sci. Rev.*, 22: 261–308

826 Neal, A. (2004) Ground-penetrating radar and its use in sedimentology: principles, problems and  
827 progress. *Earth-science reviews*, 66(3-4): 261-330

828 Ó Cofaigh, C., Evans, D.J.A. (2007) Radiocarbon constraints on the age of the maximum advance of  
829 the British-Irish Ice Sheet in the Celtic Sea. *Quaternary Science Reviews* 26 (9–10), 1197–  
830 1203

831 Ó Cofaigh, C., Weilbach, K., Lloyd, J.M., Benetti, S., Callard, S.L., Purcell, C., Chiverrell, R.C.,  
832 Dunlop, P., Saher, M., Livingstone, S.J. and Van Landeghem, K.J. (2019) Early deglaciation  
833 of the British-Irish Ice Sheet on the Atlantic shelf northwest of Ireland driven by  
834 glacioisostatic depression and high relative sea level. *Quaternary Science Reviews*, 208: 76-  
835 96

836 Pellicer, X. M., & Gibson, P. (2011). Electrical resistivity and Ground Penetrating Radar for the  
837 characterisation of the internal architecture of Quaternary sediments in the Midlands of  
838 Ireland. *Journal of Applied Geophysics*, 75(4), 638–647.  
839 <https://doi.org/10.1016/j.jappgeo.2011.09.019>

840 Pellicer, X. M., Warren, W. P., Gibson, P., & Linares, R. (2012). Construction of an evolutionary  
841 deglaciation model for the Irish midlands based on the integration of morphostratigraphic  
842 and geophysical data analyses. *Journal of Quaternary Science*, 27(8), 807–818.  
843 <https://doi.org/10.1002/jqs.2570>

844 Perkins, A. J., Brennand, T. A., & Burke, M. J. (2016). Towards a morphogenetic classification of  
845 eskers: Implications for modelling ice sheet hydrology. *Quaternary Science Reviews*, 134:  
846 19–38. <https://doi.org/10.1016/j.quascirev.2015.12.015>

847 Perkins, A.J., Brennand, T.A. and Burke, M.J. (2013) Genesis of an esker-like ridge over the  
848 southern Fraser Plateau, British Columbia: Implications for paleo-ice sheet reconstruction  
849 based on geomorphic inversion. *Geomorphology*, 190: 27-39

850 Price, R.J. (1969) Moraines, sandar, kames and eskers near Breidamerkurjökull,  
851 Iceland. *Transactions of the Institute of British Geographers*: 17-43

852 Roberts, M.C., Niller, H.P. and Helmstetter, N. (2003) Sedimentary architecture and radar facies of a  
853 fan delta, Cypress Creek, West Vancouver, British Columbia. *Geological Society, London,*  
854 *Special Publications*, 211(1): 111-126

855 Röthlisberger, H. (1972) Water pressure in intra-and subglacial channels. *Journal of*  
856 *Glaciology*, 11(62): 177-203

857 Russell, A.J., Knudsen, O., Fay, H., Marren, P.M., Heinz, J. and Tronicke, J. (2001) Morphology  
858 and sedimentology of a giant supraglacial, ice-walled, jökulhlaup channel, Skeiðarárjökull,  
859 Iceland: implications for esker genesis. *Global and Planetary Change*, 28(1-4): 193-216

860 Sambrook-Smith, G.H., Ashworth, P.J., Best, J.L., Woodward, J. and Simpson, C.J. (2006) The  
861 sedimentology and alluvial architecture of the sandy braided South Saskatchewan River,  
862 Canada. *Sedimentology*, 53(2): 413-434

863 Saunderson, H.C. (1977) The sliding bed facies in esker sands and gravels: a criterion for full-pipe  
864 (tunnel) flow? *Sedimentology*, 24(5):623-638

865 Schoof, C. (2010) Ice-sheet acceleration driven by melt supply variability. *Nature*, 468(7325): 803

866 Shreve, R. L. (1985). Esker characteristics in terms of glacier physics, Katahdin esker system,  
867 Maine. *Geological Society of America Bulletin*, 96(5), 639–646.  
868 [https://doi.org/10.1130/0016-7606\(1985\)96<639:ECITOG>2.0.CO;2](https://doi.org/10.1130/0016-7606(1985)96<639:ECITOG>2.0.CO;2)

869 Smith, M.J. and Knight, J. (2011) Palaeoglaciology of the last Irish Ice Sheet reconstructed from  
870 striae evidence. *Quaternary Science Reviews*, 30(1-2): 147-160

871 Sollas, W.J. (1896) A map to show the Distribution of Eskers in Ireland. *Sci. Trans. R. Dublin Soc*,  
872 2(5): 785-822.

873 Stearns, L.A., Smith, B.E. and Hamilton, G.S. (2008). Increased flow speed on a large East  
874 Antarctic outlet glacier caused by subglacial floods. *Nature Geoscience*, 1(12), 827-831.

875 Storrar, R. D., Evans, D. J. A., Stokes, C. R., & Ewertowski, M. (2015). Controls on the location,  
876 morphology and evolution of complex esker systems at decadal timescales,  
877 Breidamerkurjökull, southeast Iceland. *Earth Surface Processes and Landforms*, 40(11),  
878 1421–1438. <https://doi.org/10.1002/esp.3725>

879 Storrar, R.D., Ewertowski, M., Tomczyk, A.M., Barr, I.D., Livingstone, S.J., Ruffell, A., Stoker,  
880 B.J. and Evans, D.J. (2020) Equifinality and preservation potential of complex  
881 eskers. *Boreas*, 49(1), 211-231.

882 Storrar, R.D., Stokes, C.R. and Evans, D.J. (2013) A map of large Canadian eskers from Landsat  
883 satellite imagery. *Journal of maps*, 9(3): 456-473

884 Storrar, R.D., Stokes, C.R. and Evans, D.J. (2014a) Morphometry and pattern of a large sample (>  
885 20,000) of Canadian eskers and implications for subglacial drainage beneath ice  
886 sheets. *Quaternary Science Reviews*, 105: 1-25

887 Storrar, R.D., Stokes, C.R. and Evans, D.J. (2014b) Increased channelization of subglacial drainage  
888 during deglaciation of the Laurentide Ice Sheet. *Geology*, 42(3): 239-242

889 Stroeve, A. P., Hättestrand, C., Kleman, J., Heyman, J., Fabel, D., Fredin, O., Goodfellow, B. W.,  
890 Harbor, J. M., Jansen, J. D., Olsen, L., Caffee, M. W., Fink, D., Lundqvist, J., Rosqvist, G.  
891 C., Strömberg, B. & Jansson, K. N. (2016) Deglaciation of Fennoscandia. *Quaternary*  
892 *Science Reviews*, 147, 91-121.

893 Walther, J. (1894) Einleitung in die Geologie als historische Wissenschaft. In *Lithogenesis der*  
894 *Gegenwart*. Jena: G. Fischer, Bd. 3: 535–1055.

895 Warren, W.P. and Ashley, G.M. (1994) Origins of the ice-contact stratified ridges (eskers) of  
896 Ireland. *Journal of Sedimentary Research*, 64(3a): 433-449

897 Wilson, P., Ballantyne, C.K., Benetti, S., Small, D., Fabel, D. and Clark, C.D. (2019) Deglaciation  
898 chronology of the Donegal Ice Centre, north-west Ireland. *Journal of Quaternary Science*,  
899 34(1): 16-28

900 Winsemann, J., Asprion, U., Meyer, T. and Schramm, C. (2007) Facies characteristics of Middle  
901 Pleistocene (Saalian) ice-margin subaqueous fan and delta deposits, glacial Lake Leine, NW  
902 Germany. *Sedimentary Geology*, 193(1-4): 105-129

903 Winsemann, J., Hornung, J.J., Meinsen, J., Asprion, U., Polom, U., Brandes, C., BUßMANN,  
904 M.I.C.H.A.E.L. and Weber, C. (2009) Anatomy of a subaqueous ice-contact fan and delta  
905 complex, Middle Pleistocene, North-west Germany. *Sedimentology*, 56(4): 1041-1076

906 Winsemann, J., Lang, J., Polom, U., Loewer, M., Igel, J., Pollok, L. and Brandes, C. (2018) Ice-  
907 marginal forced regressive deltas in glacial lake basins: geomorphology, facies variability  
908 and large-scale depositional architecture. *Boreas*, 47(4): 973-1002

909 Wright, A. P., Siegert, M. J., Le Brocq, A. M., & Gore, D. B. (2008). High sensitivity of subglacial  
910 hydrological pathways in Antarctica to small ice-sheet changes. *Geophysical Research*  
911 *Letters*, 35(17), 1–5. <https://doi.org/10.1029/2008GL034937>

912 Zwally, H.J., Abdalati, W., Herring, T., Larson, K., Saba, J. and Steffen, K. (2002) Surface melt-  
913 induced acceleration of Greenland ice-sheet flow. *Science*, 297(5579): 218-222

914

915

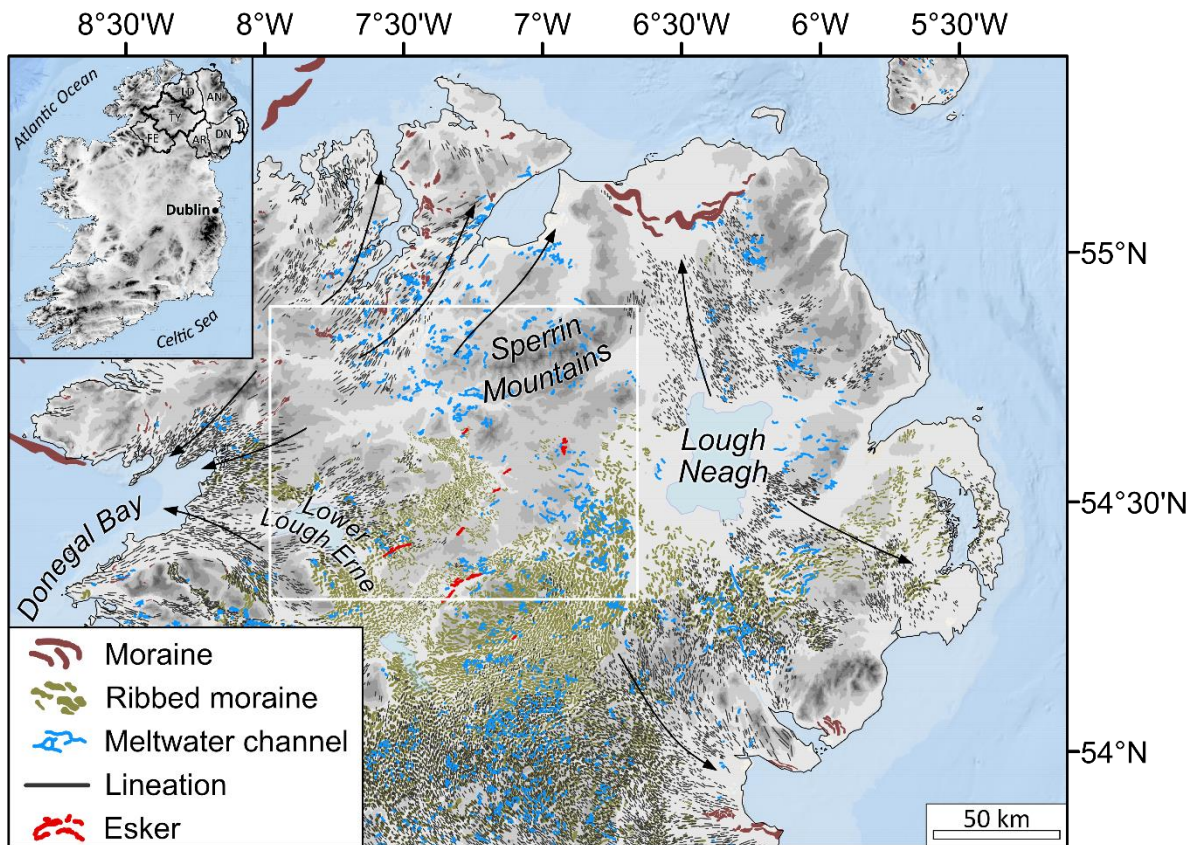


Figure 1. The distribution of mapped glacial landforms within the BRITICE v2 database across Northern Ireland (Clark *et al.*, 2018). Lineations include Mega-Scale Glacial Lineations (MSGL) and drumlins. Major ice flow directions during the LGM are indicated by the black arrows. The white box indicates the study area.


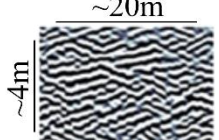
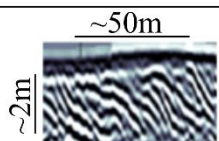
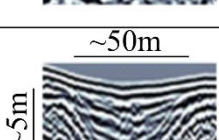
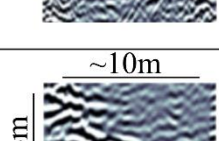
Facies type	Radar facies example	Facies characteristics	Facies interpretation
Esker ridge facies		Radar Facies 1: Chaotic, discontinuous reflectors.	Coarse gravel deposited subglacially under high flow velocities (Burke <i>et al.</i> , 2015)
		Radar Facies 2: Sub-horizontal moderately continuous reflectors	Vertical accretion of sandy material (Burke <i>et al.</i> , 2012)
		Radar Facies 3: Low-angle dipping reflections	Delta foresets composed of sand and gravel (Burke <i>et al.</i> , 2010)
		Radar Facies 4: Concave-up, bowl-shaped reflectors	Erosional trough fills (Perkins <i>et al.</i> , 2016)
Post-glacial facies		Radar Facies 5: Attenuated, horizontal reflections	Post-glacial peat infill (Jol and Smith, 1991)

Table 1. Summary of key radar facies observed along the Evishanoran Esker, including both glaciofluvial and post-glacial features. Further description and interpretation of radar facies is presented in Section 4.2.1.



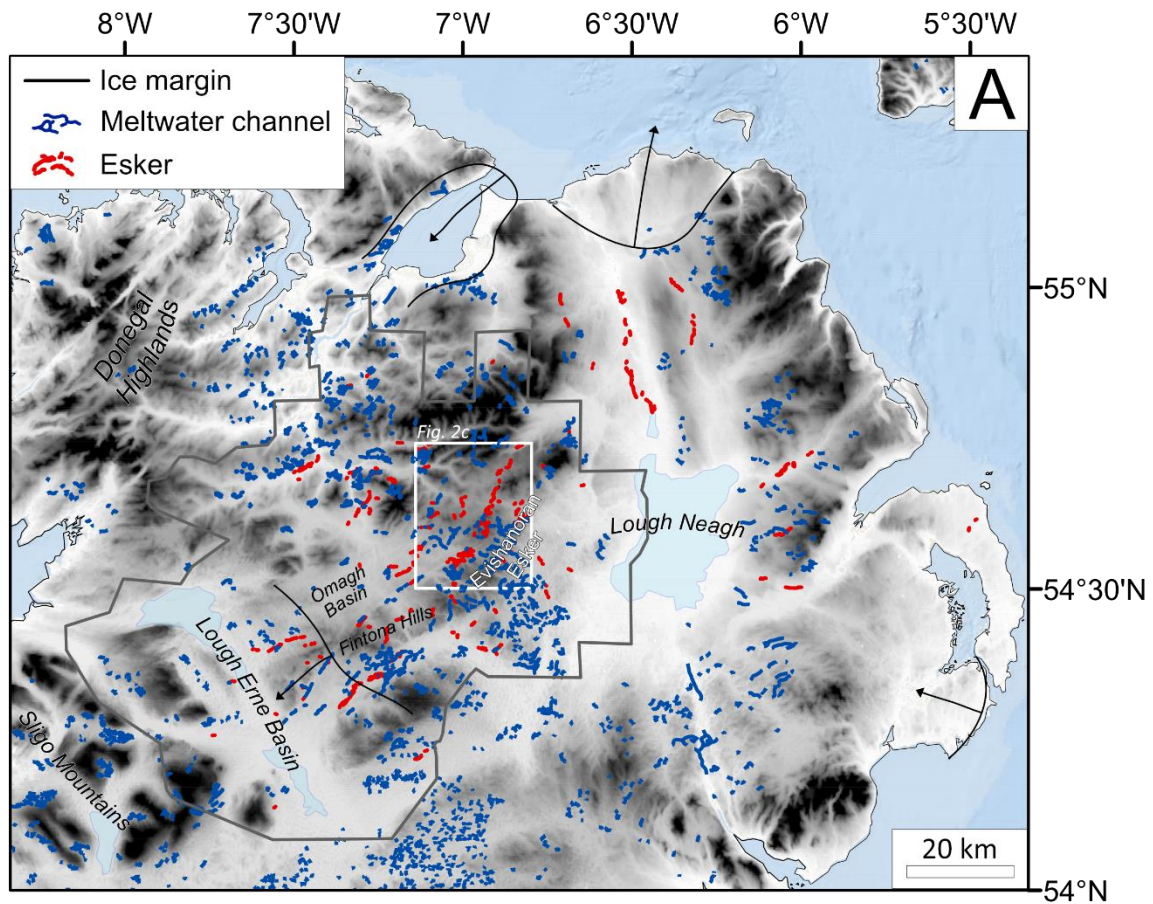


Figure 2. (a) An updated map of the meltwater landforms of Northern Ireland, including features mapped in this study. Meltwater channels from the BRITICE v2 compilation are also included (Clark *et al.*, 2018). Note the occurrence of a large esker system to the west of Lough Neagh, unreported in the BRITICE database. Ice margin positions are adapted from Greenwood and Clark (2009b), with arrows showing ice margin retreat direction. The grey box indicates the extent of high-resolution ( $\sim 0.4$  m) DSM coverage used within this study and shown in Figure 2b.



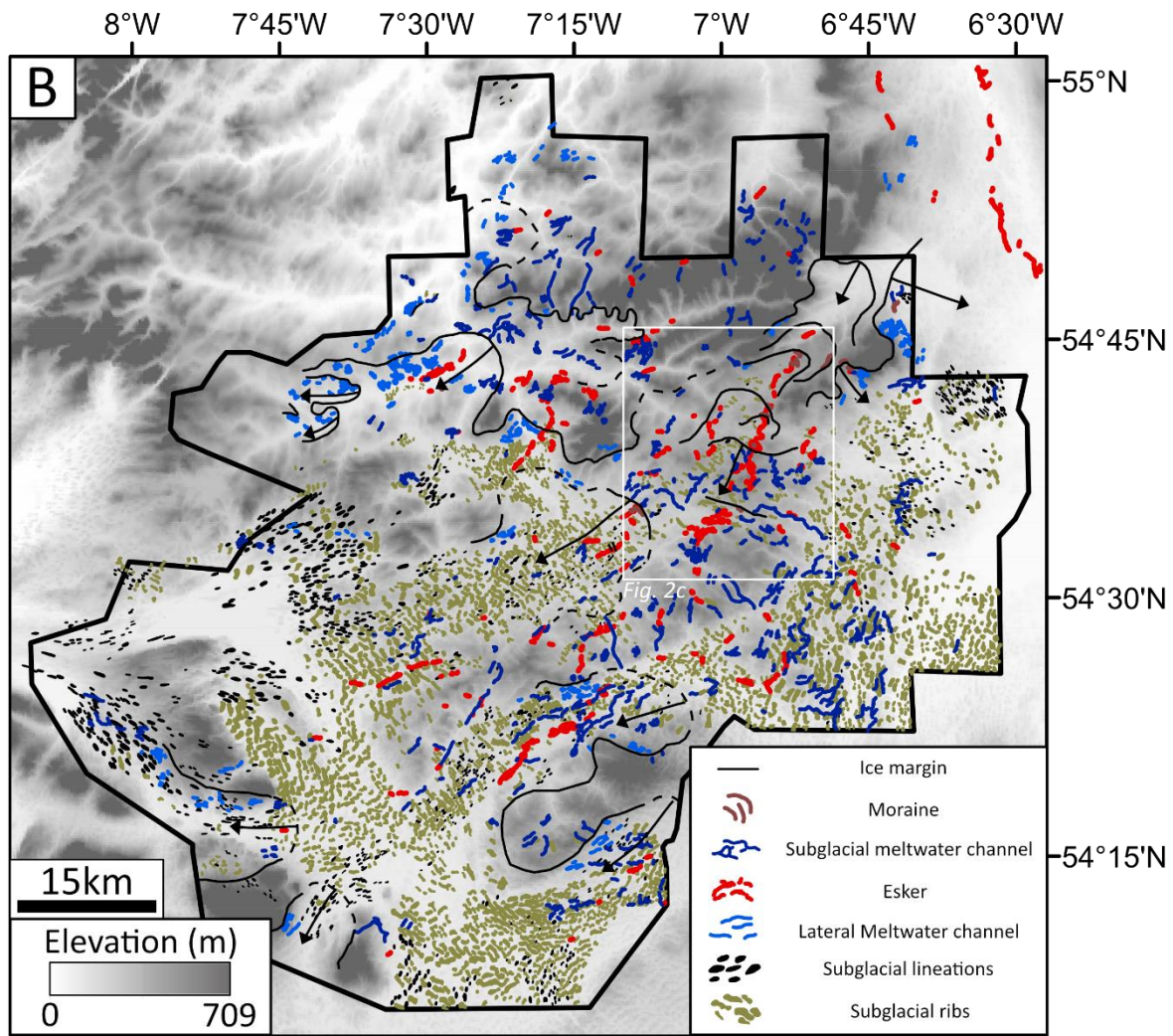


Figure 2. (b) Glacial geomorphology of SW Northern Ireland based on a 0.4m DSM. Schematic ice margin positions (black lines) have been drawn based on esker morphology, fan deposits, lateral meltwater channels and moraines. Dashed black lines indicate areas of lower certainty in ice margin position. Black arrows indicate ice margin retreat directions. The black outline indicates the extent of DSM coverage.

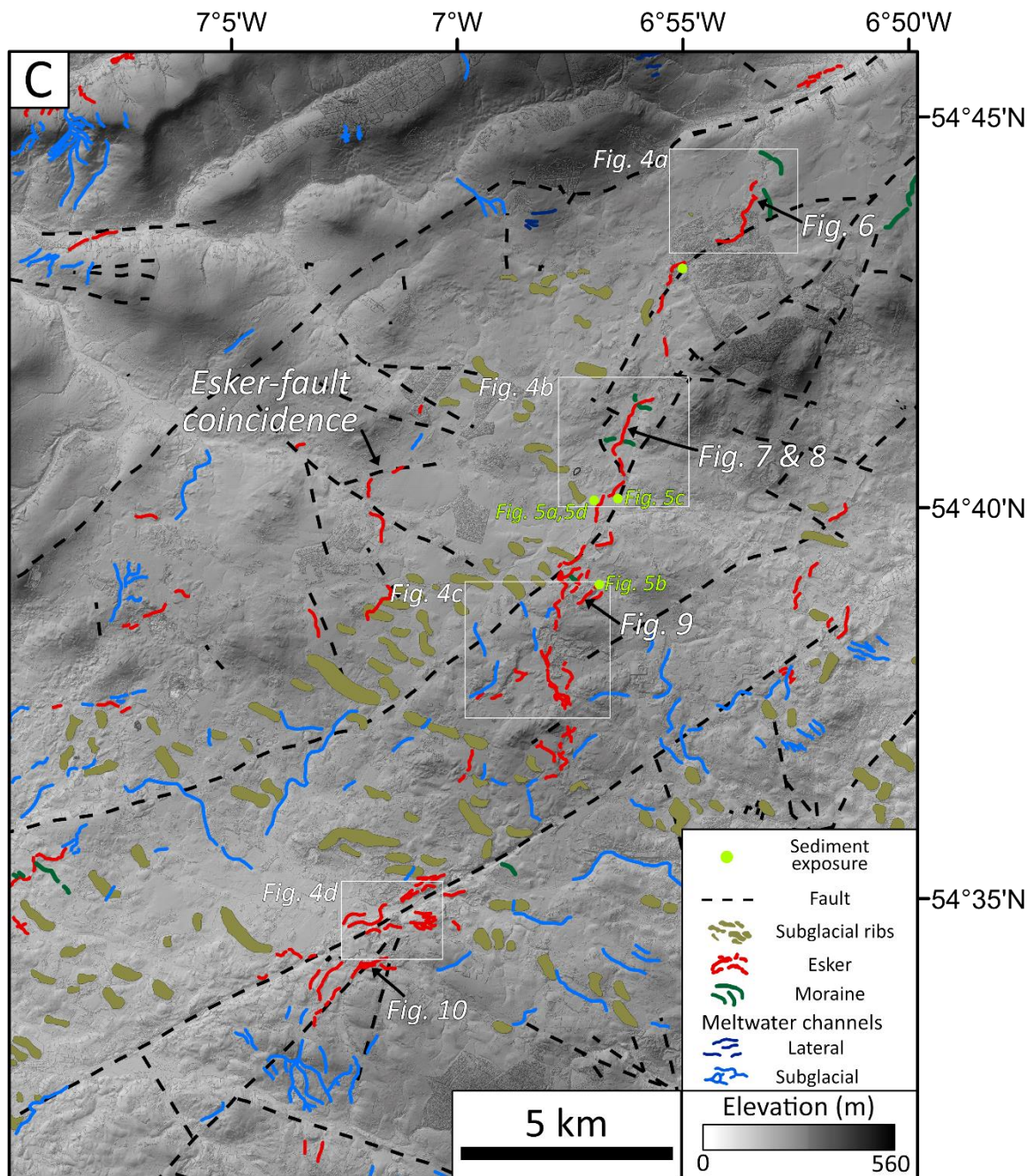


Figure 2. (c) The esker system in County Tyrone, annotated with the location of investigated sediment exposures. Note the coincidence of the southern esker system with a large SW-NE trending fault, while some eskers in the northwest demonstrate dramatic changes in orientation to follow fault lines. White boxes highlight features detailed within Figure 4. Yellow text indicates which photographs from Figure 5 relate to each sediment exposure. Geological faulting data is based on the 10K geology dataset, reproduced with the permission of the Geological Survey of Northern Ireland. Crown Copyright 2018.





Figure 3. Photographs detailing the morphology of the Evishanoran Esker. (A) Looking east along a round-crested ridge within the complex, multi-ridge esker in the southern sector ( $54.571^{\circ}\text{N}$ ,  $-7.041^{\circ}\text{E}$ ). (B) An esker ridge ending in a fan-shaped deposit within the central sector of the esker complex, formed by water flow down the hill from the right of the image ( $54.650^{\circ}\text{N}$ ,  $-6.953^{\circ}\text{E}$ ). (C) A ridge along the Esker Road within the northern sector ( $54.683^{\circ}\text{N}$ ,  $-6.942^{\circ}\text{E}$ ). Radar surveys revealed peat infilling around the ridge, masking the true esker size. (D) Variations in ridge morphology towards the termination of the northern sector ( $54.734^{\circ}\text{N}$ ,  $-6.893^{\circ}\text{E}$ ).

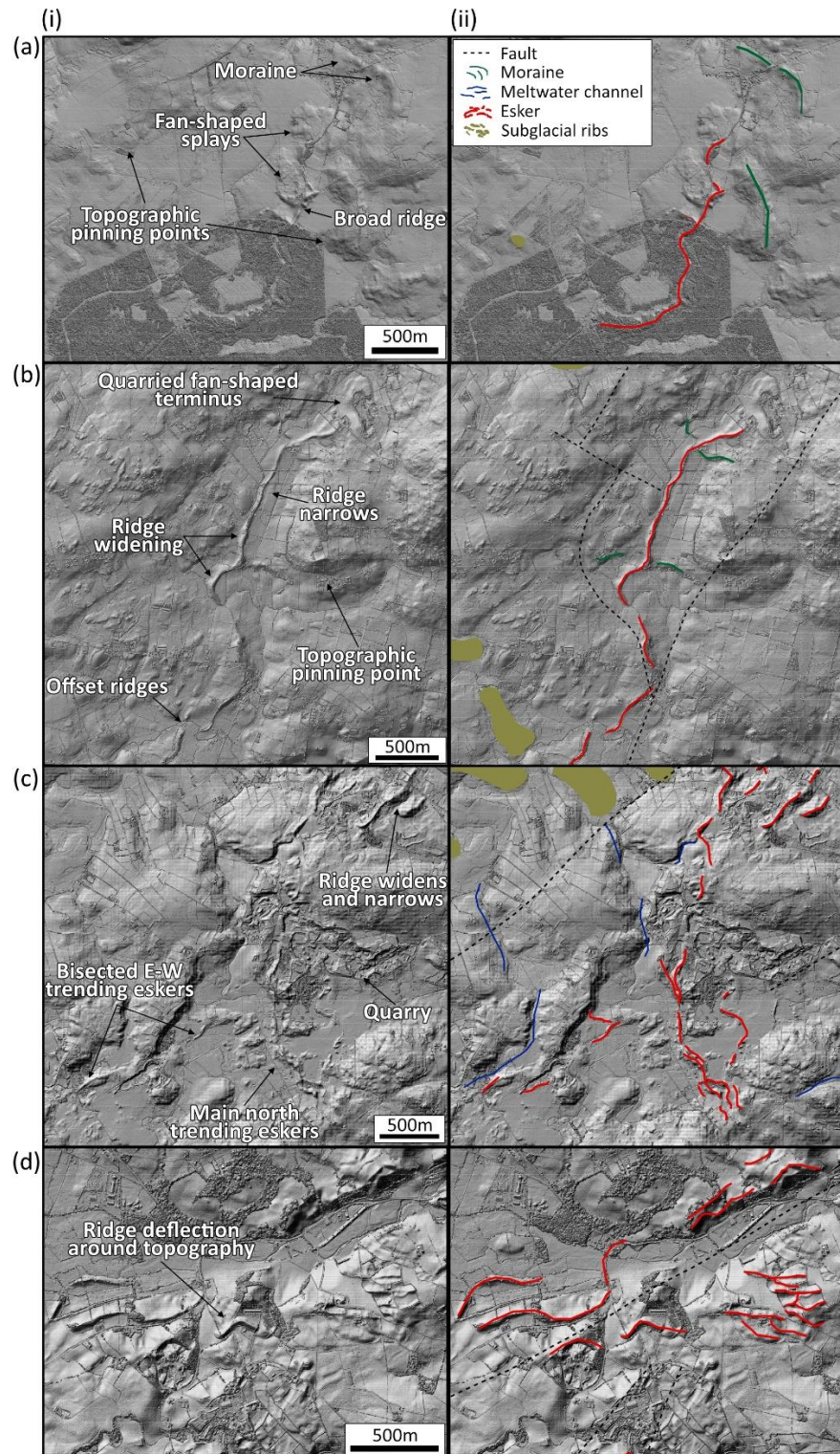


Figure 4. Hillshaded DEM detailing key morphological characteristics of the Evishanoran Esker. (a) Widening of the esker ridge towards the terminus of the simple system in the northern sector, (b) Offset ridges at the initiation of the simple system in the northern sector, (c) Cross-cutting of east trending ridges by the main north trending ridge within the complex esker system in the central sector of the esker complex, (d) Deflection of ridges around a topographic obstacle (possible bedrock or earlier drumlin) within the southern sector.

	<b>Southern sector</b>	<b>Central sector</b>	<b>Northern sector</b>
<b>Planform</b>	Complex, multi-ridge	Complex, tributary system	Simple
<b>Average ridge length (m)</b>	357	334	678
<b>Sinuosity</b>	1.17	1.21	1.20
<b>Topographic context</b>	Normal slope through undulating topography	Normal slope through hilly topography	Reverse slope through a uniform valley bottom
<b>Relative relief (m)</b>	~7	~6	~10-15
<b>Total esker length (km)</b>	~6.5 (36 ridges)	~7.4 (39 ridges)	~9.3 (10 ridges)

960 Table 2. The key morphological characteristics of the complex esker system in County Tyrone. The  
961 distance along the crestline of each ridge was measured to define the average ridge length. Esker  
962 sinuosity was calculated for each individual ridge by dividing the esker ridge length by the straight-line  
963 distance from esker initiation to terminus, and is presented as a mean for each sector.



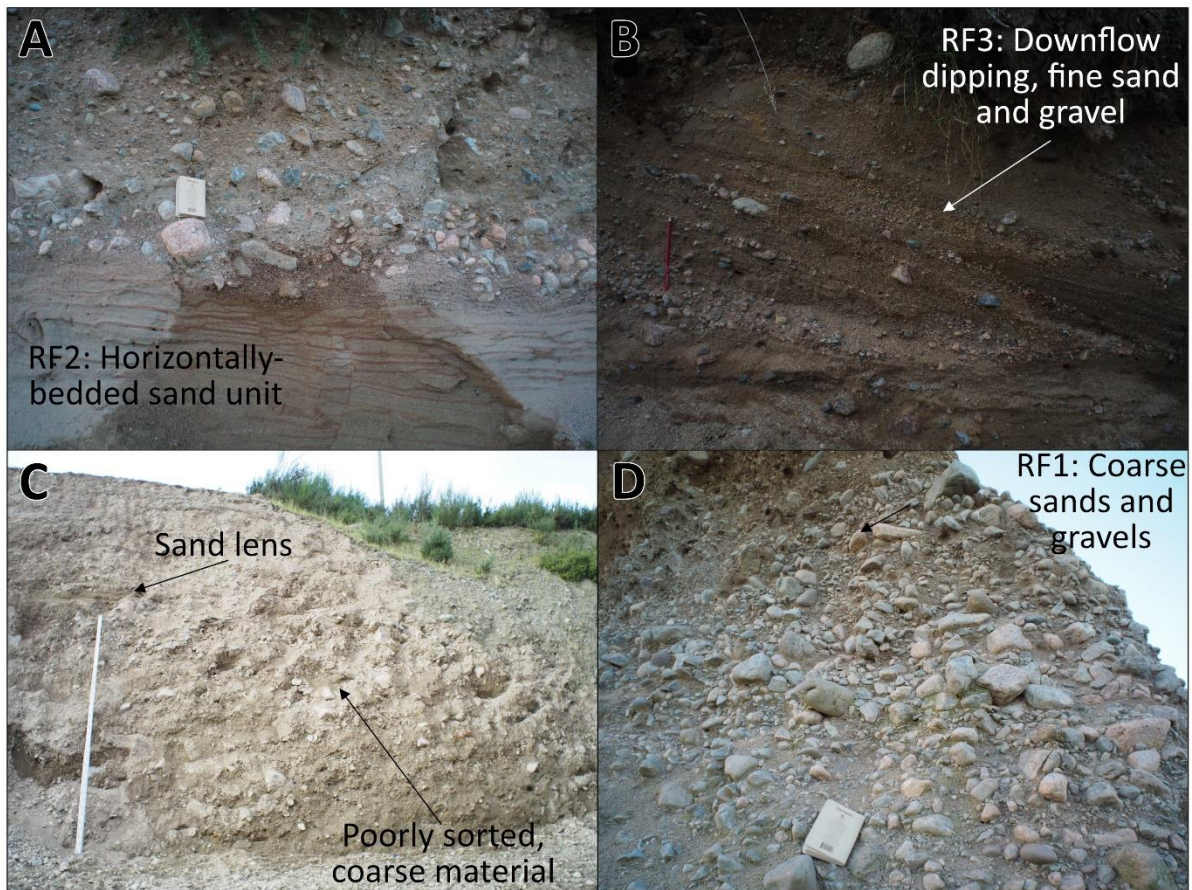


Figure 5. (a) Sediment exposure from the southern-end of the northern sector, consisting of a series of horizontally stratified sands (RF2), overlain by a poorly sorted sand and gravel unit (54.668°N, -6.950°E). (b) Sediment exposure within the central, complex esker system, dominated by a series of downflow-dipping sands and gravelly sands associated with RF3 (54.650°N, -6.953°E). (c) Quarried section of the single esker ridge system to the north of (a). Facies consist of coarse, diamictic material with boulders up to 50 cm (54.672°N, -6.941°E). (d) Poorly-sorted sand and gravel units observed within the northern sector, commonly associated with RF1 (54.668°N, -6.950°E).

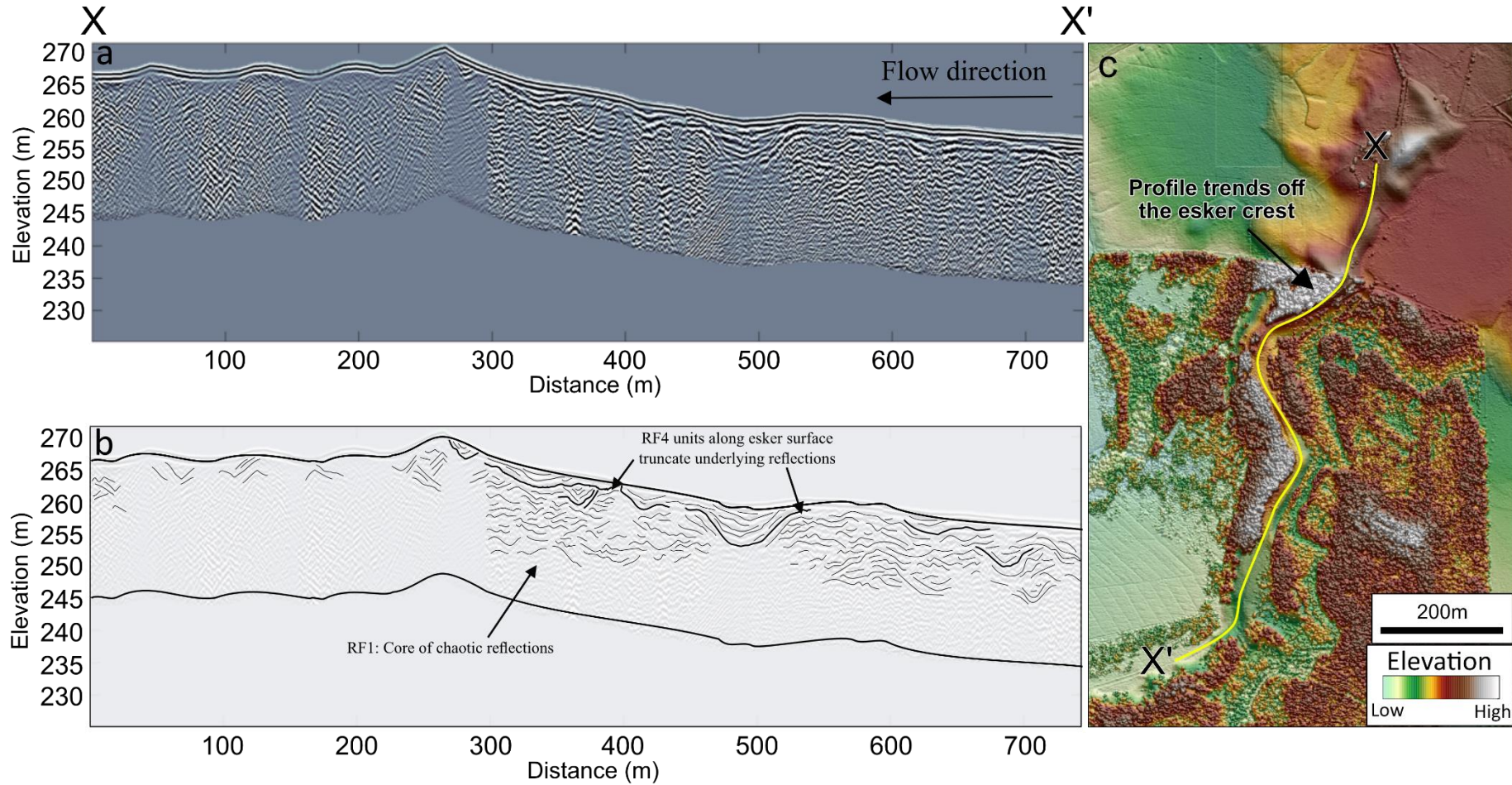


Figure 6. (a) 100 MHz long-profile radar survey along the crest of a single ridge esker towards the NE terminus of the County Tyrone Esker, the location of the survey line is presented in Figure 2. Ice flow direction is indicated by the black arrow. (b) shows an interpreted radar profile derived through the tracing of key reflections. (c) Inset figure showing the detailed esker morphology and the location of radar survey (yellow line).



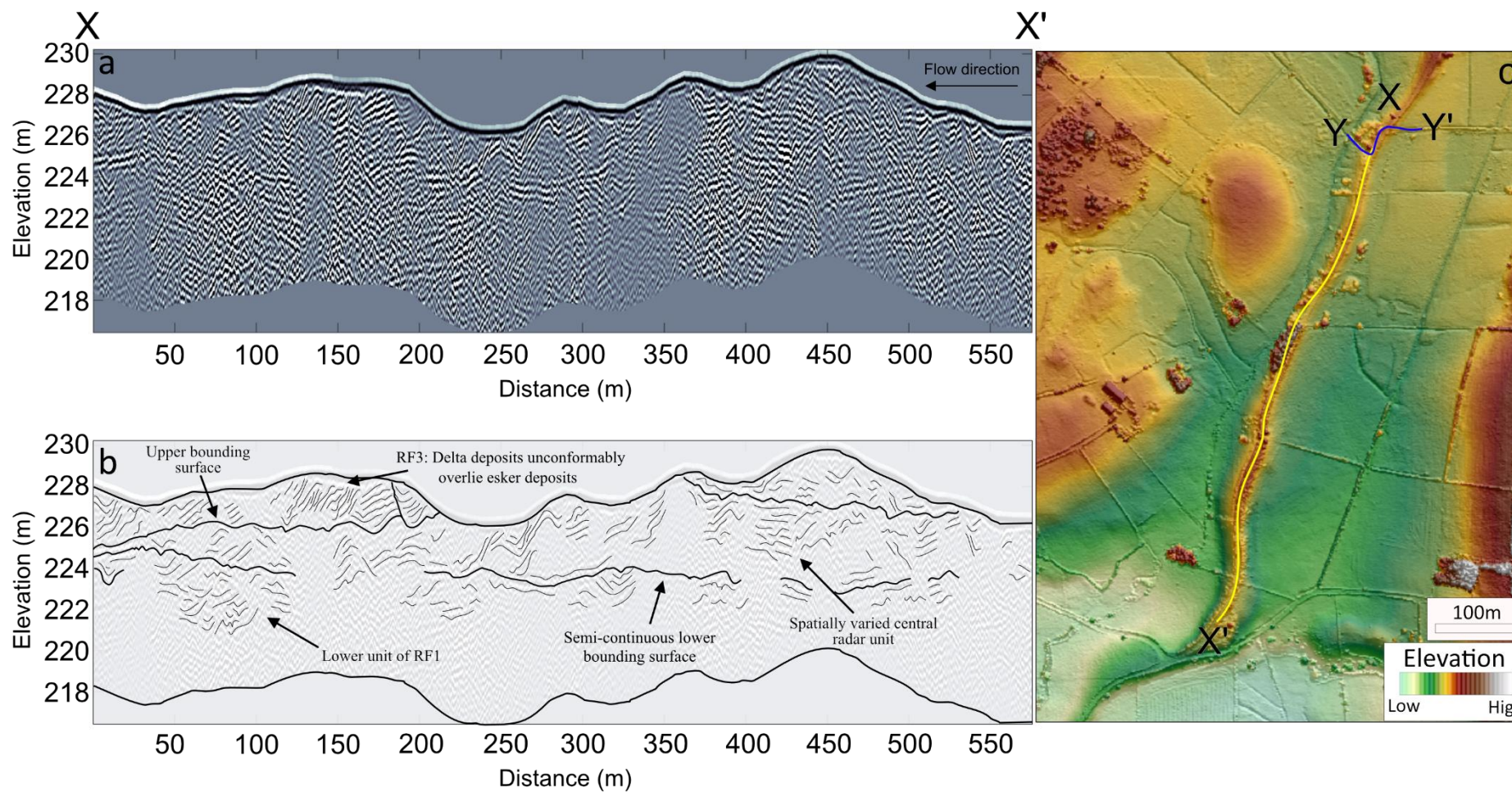


Figure 7. (a) 160 MHz long-profile radar survey along the crest of a single ridge esker near the initiation of the simple system, the location of the survey line is presented in Figure 2. Ice flow direction is indicated by the black arrow. (b) shows an interpreted radar profile derived through the tracing of key reflections. (c) Inset figure showing the detailed esker morphology and the location of radar surveys for Figure 7 (yellow line) and Figure 8 (blue line).



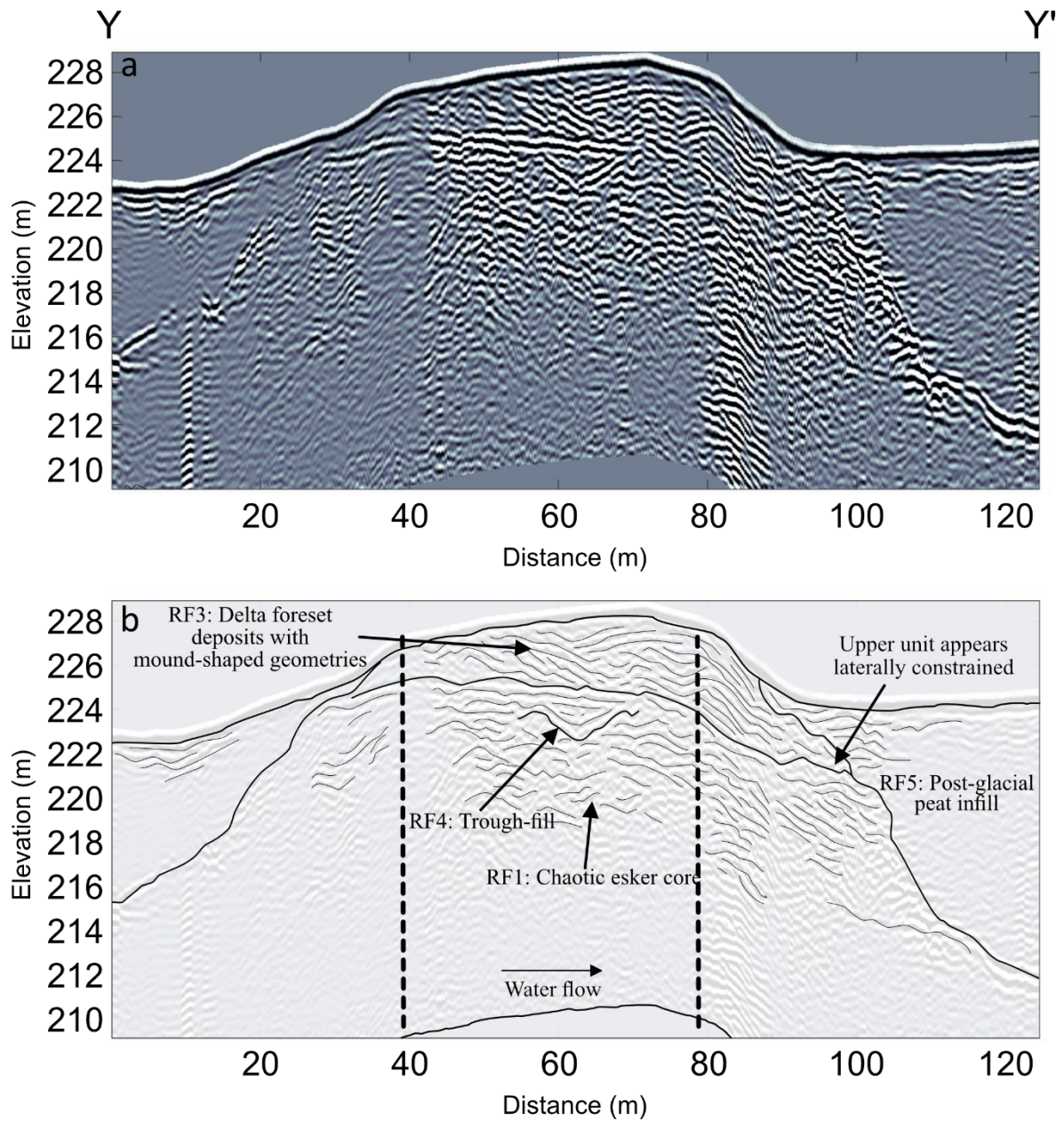


Figure 8. (a) 160 MHz cross-profile radar survey of a single ridge esker near the initiation of the northern sector. (b) shows an interpreted radar profile derived through the tracing of key reflections. Vertical dashed lines indicate the portion of the radar survey which travelled along the esker ridge. The location of the radar profile is indicated on Figure 7c by a blue line.

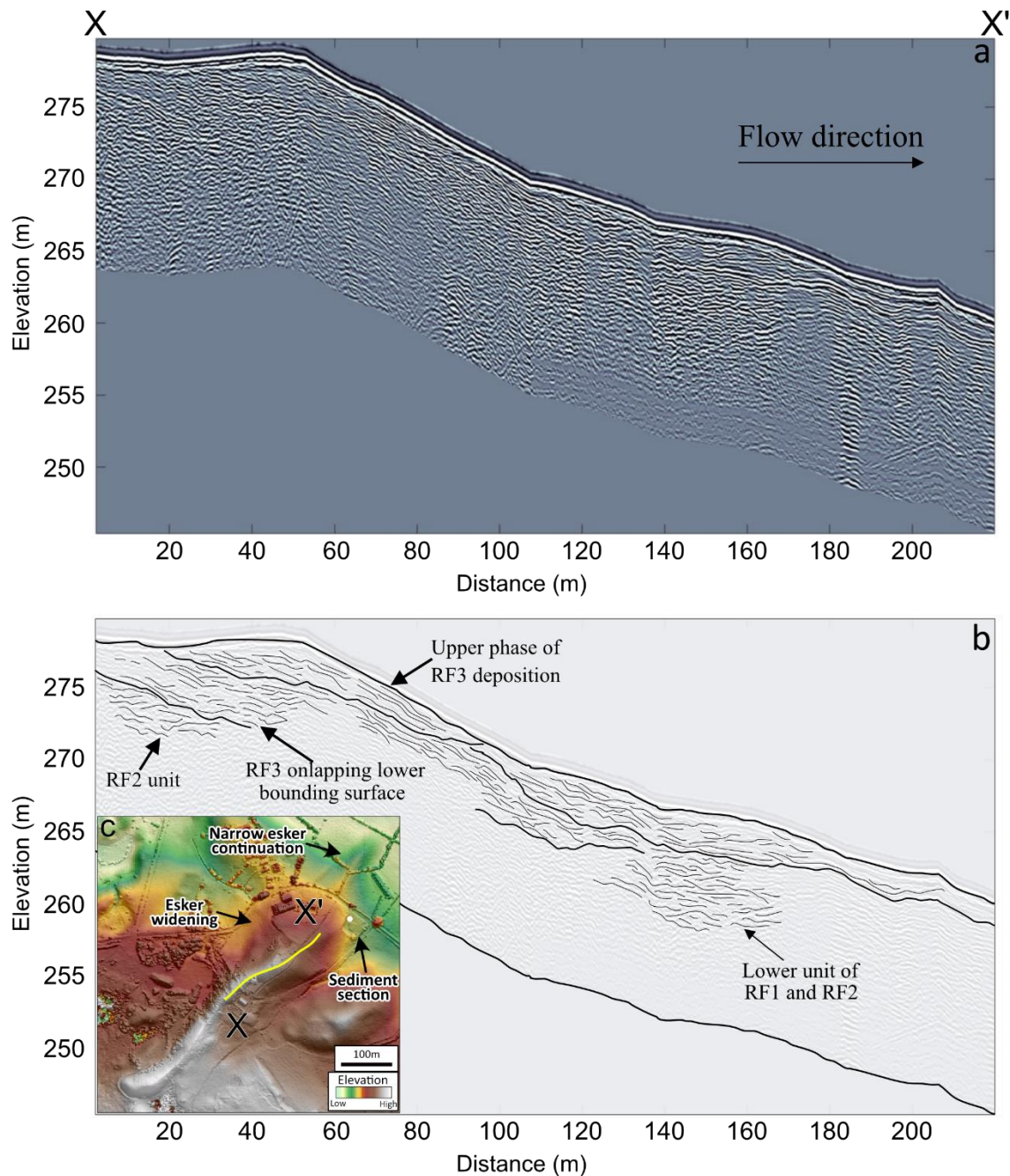
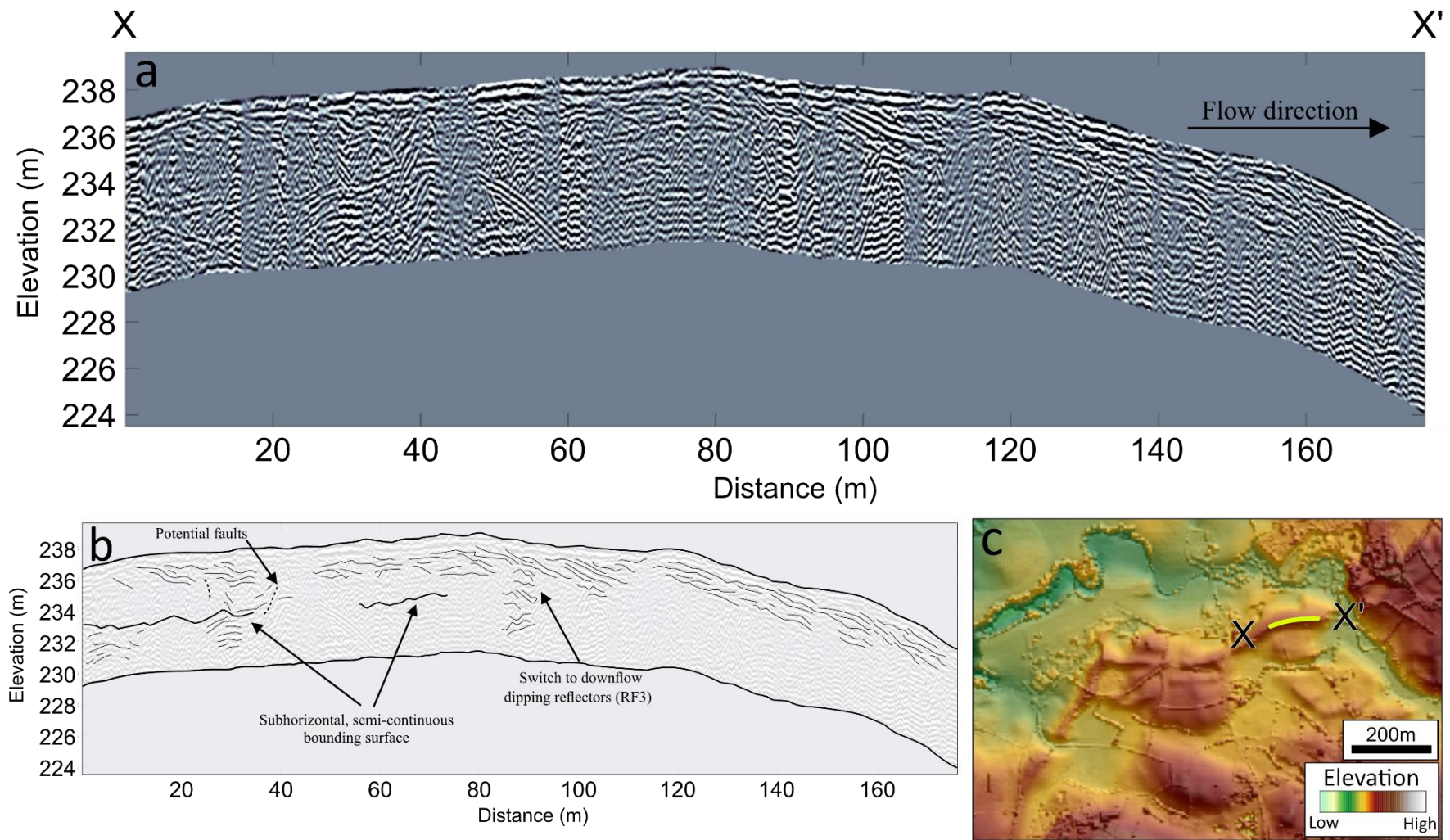


Figure 9. (a) 160 MHz radar profile along the crest of an esker within the complex central sector. Ice flow direction is indicated by the black arrow. (b) shows an interpreted radar profile derived through the tracing of key reflections. (c) Inset figure showing the detailed esker morphology and the location of radar survey (yellow line), while the labelled sediment section (white dot) is photographed in Figure 5b.





996  
 997 Figure 10. (a) 160 MHz radar profile along the crest of an esker within the southern sector. Ice flow direction is indicated by the black arrow. (b) shows an  
 998 interpreted radar profile derived through the tracing of key reflections. (c) Inset figure showing the detailed esker morphology and the location of radar survey  
 999 (yellow line).

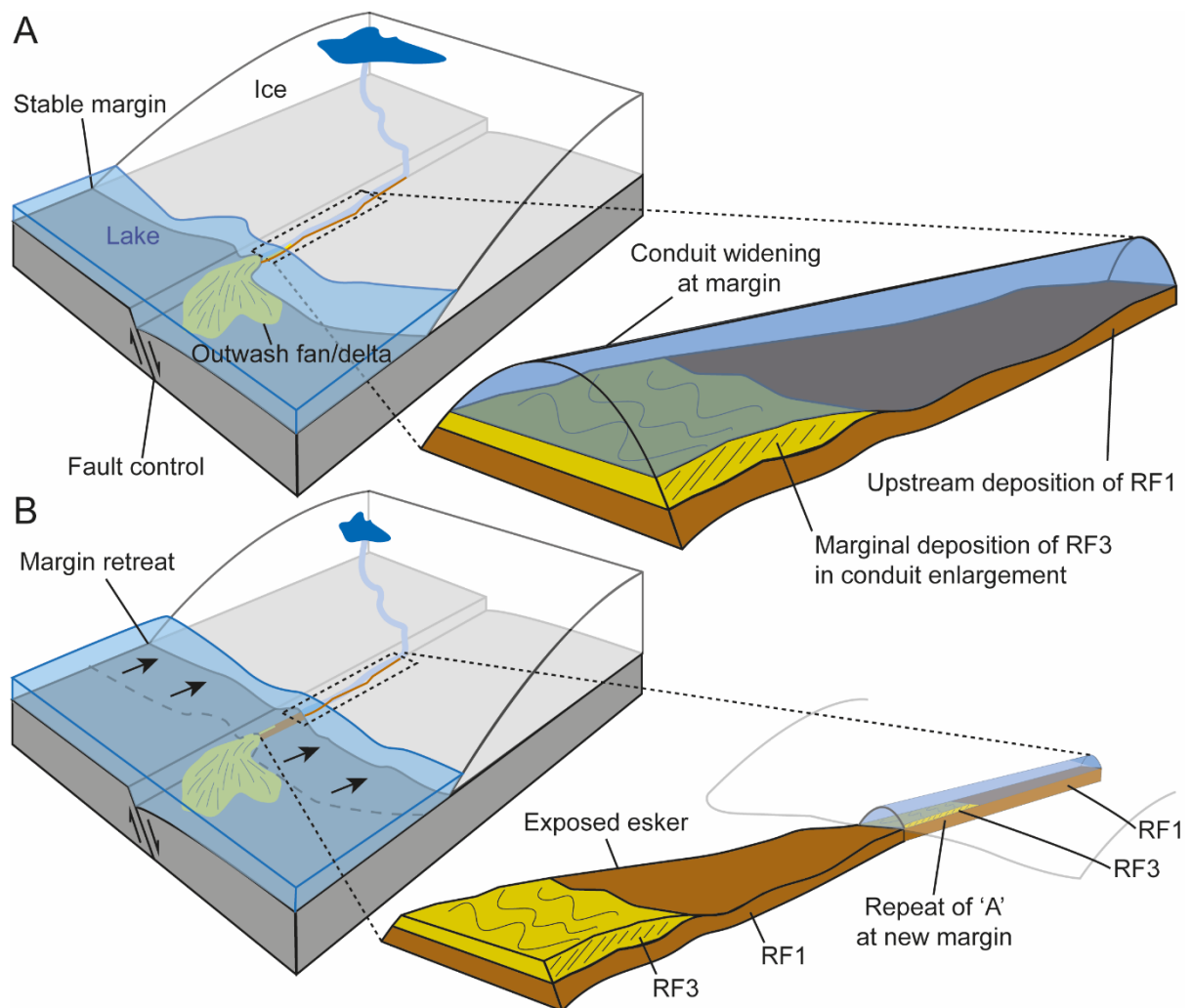


Figure 11. A conceptual model of the time-transgressive esker deposition. (a) Delta foresets are deposited in a proglacial lake at the ice sheet margin due to conduit widening, while coarser material is deposited up-ice in the subglacial conduit. (b) Ice margin retreat leads to the deposition of foresets on top of the core of esker material.